plates and solidified at room temperature. Paper filters (ϕ = 6 mm) containing extracts of the culture broth to be tested were put on the plates and the plates were incubated at 30 °C for several days.

2.3. Purification of fumagillin from a producing fungal strain

Fumagillin was isolated from the culture broth of a producing fungal strain using bioassay-guided purification procedures. The structure of fumagillin was determined by the physico-chemical properties, detailed ^{1}H and ^{13}C NMR analysis, and mass spectroscopy [19].

2.4. Synthesis of TNP470 and biotinylated fumagillin

TNP470 was synthesized from fumagillin as described previously [20]. Biotinylated fumagillin was synthesized by a coupling reaction via the carboxyl group of fumagillin using an activated biotin reagent (Pierce). The structures of TNP470 and biotinylated fumagillin were determined by their physico-chemical properties, detailed ^{1}H and ^{13}C NMR analysis, and mass spectroscopies. Biotinylated fumagillin was confirmed to be effective in MT-Vpr1 cells although it was weaker than the original.

2.5. Human cell culture and immunological techniques

Cell culture, synchronization and FACS analysis of MT-Vpr1 cells, a HeLa derived cell line with zinc inducible Vpr expression plasmids, and immunological detection of Vpr in the cells were as described [16]. Human embryonic kidney (HEK) 293 cells expressing SV40 large T antigen (293T) were propagated in DMEM medium supplemented with 10% FCS. Human primary monocytes and differentiated macrophages were obtained from peripheral blood mononuclear cells of healthy donors as described [21].

2.6. Preparation of viruses

To generate the single-round replication incompetent luciferase reporter virus stocks (NL-Luc-E$^-$R$^+$ or NL-Luc-E$^-$R$^-$)[2], 293T cells were co-transfected with the proviral DNAs (obtained from Dr. Nathaniel Landau through the AIDS Research and Reference Reagent Program) and plasmids encoding vesicular stomatitis virus envelope protein (pCMV-VSV-G-RSV-Rev). Culture supernatants were harvested at 60 h after the transfection and titrated.

2.7. Infectivity assays

Primary macrophages in 24 well plates were inoculated with VSV-G pseudotyped reporter viruses (NL-Luc-E$^-$R$^+$(VSV-G) or NL-Luc-E$^-$R$^-$(VSV-G); 1.5 ng of $p24^{gag}$ antigen), cultured in the absence or presence of the drug (fumagillin or TNP470) for 6 days, harvested, lysed in luciferase assay substrate (Promega) and assayed for luciferase activities using Wallac ARVO SX 1420 (Perkin–Elmer).

3. Results and discussion

3.1. Isolation of Vpr inhibitors using budding yeast cells

To isolate small molecules that inhibit the activity of Vpr, we have established a screening system using budding yeast cells expressing Vpr. As shown in Fig. 1A, yeast cells with copper-inducible Vpr expression plasmids [22] were embedded in agar plates containing the inducer ($CuSO_4$). Then, paper filters containing extracts of broth from cultured microorganisms (fungi, actinomycetes or bacteria) were put on agar plates, and the plates were incubated at 30 °C for several days. Since Vpr strongly inhibits the growth of yeast cells [22], no significant growth was usually detected even after 4–5 days of incubation. However, very occasionally, significant growth could be detected surrounding the paper filters, indicating that the culture broth extracts on the filters have an activity that antagonizes the action of Vpr (Fig. 1B). As a result of our extensive screening program, we have purified the active compound and identified it as fumagillin (Fig. 1C and D), a compound known to be a potent inhibitor of angiogenesis [11]. Commercially available fumagillin (Sigma) had specific activity similar to that of our purified compound (not shown). The activity of fumagillin could also be detected when a galactose inducible system was used for Vpr expression (not shown), suggesting that this compound reverses the action of Vpr itself rather than the expression of Vpr by copper inducible system (see below).

3.2. Effect of fumagillin and TNP470 on Vpr induced cell cycle arrest in HeLa cells

Next, we examined the ability of fumagillin to antagonize Vpr function in human cells. As described above, one of the characteristic functions of Vpr in human cells is induction of the cell cycle arrest at G2 phase [23,24]. We previously established a HeLa derived cell line (MT-Vpr1) stably transfected with a zinc-inducible Vpr expression vector [16]. In this cell line, induction of Vpr expression arrests cell cycle at G2 phase in more than half of the total cells a day after addition of the inducer (Fig. 2A, Zn). When fumagillin (10 ng/ml) was added before the addition of zinc, the G2 arrested population was

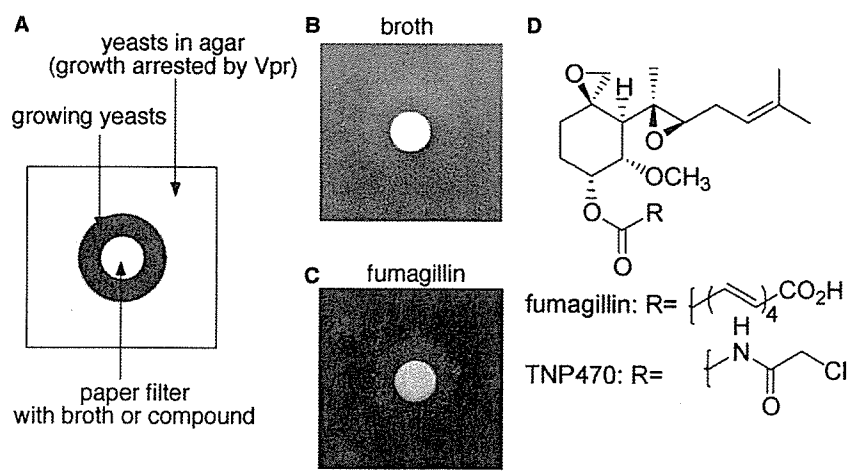

Fig. 1. Screening system to isolate Vpr inhibitors. (A) Schematic presentation of Vpr screening system. Budding yeast cells expressing Vpr were embedded in agar plates containing inducer (copper). Paper filters with broths or compounds to be tested were put on the plates. Only the yeasts surrounding filters that contain Vpr inhibitors were able to grow. (B,C) Growing yeasts surrounding filters containing 10 μl of extract from the culture broth of a fungus with Vpr inhibitory activity (B) or purified fumagillin (C; 2 mg/ml, 10 μl). Plates were incubated for 4 days at 30 °C. (D) Chemical structures of fumagillin and TNP470.

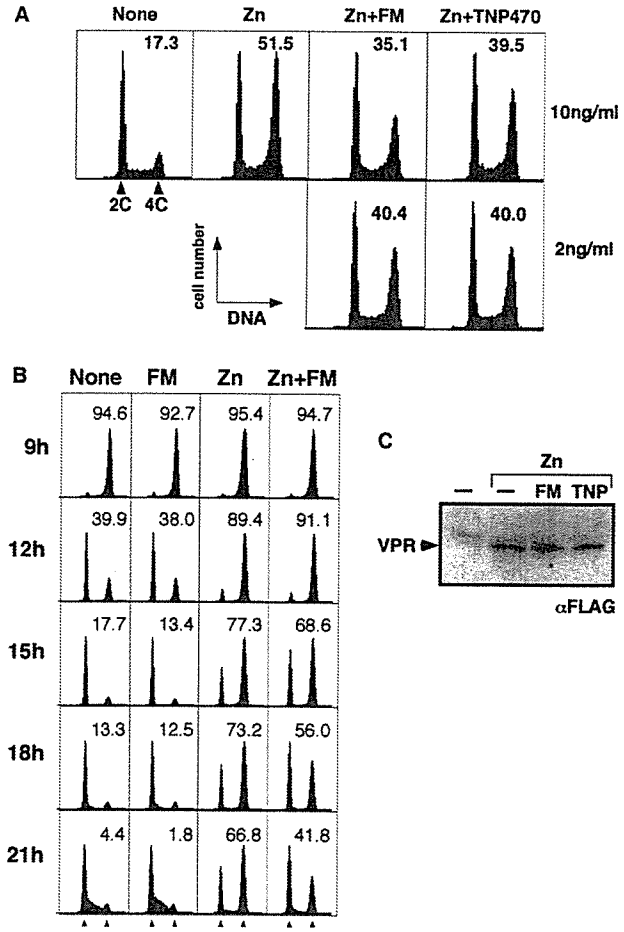

Fig. 2. Fumagillin and TNP470 inhibit Vpr activity in HeLa cells. (A) Thirty minutes before the addition of zinc, fumagillin (FM) or TNP470 was added to MT-Vpr1 cells at the concentrations described. Cells were cultured for a day in the presence or absence of zinc (Zn; 150 μM) and harvested for FACS analysis. Numbers in the figures represent the percentage of cells with 4C DNA contents. (B) Mt-Vpr1 cells were synchronized at G1/S border [16], then released in the presence or absence of zinc (Zn; 150 μM) and/or fumagillin (FM; 10 ng/ml). Zinc and fumagillin were added at 2 and 1 h before the release, respectively. Numbers in the figures represent the percentage of cells with 4C DNA contents. (C) Cells as in (A) were cultured for 6 h and harvested for western analysis to detect FLAG-Vpr expression [16]. Drugs were added at 10 ng/ml.

significantly reduced (Fig. 2A, Zn + FM). Thus, fumagillin can partially inhibit the action of Vpr in mammalian cells as well. The effect of higher doses (100 ng/ml and 1 μg/ml) of fumagillin on the action of Vpr was almost similar to that at 10 ng/ml in this system (not shown).

A synthetic analog of fumagillin, TNP470 (AGM-1470; Fig. 1D) is a more potent angiogenesis inhibitor [11]. However, the ability of TNP470 to antagonize Vpr function was similar to or less than that of fumagillin (Fig. 2A, Zn + TNP470). Thus, fumagillin seems to override Vpr-dependent cell cycle arrest in a manner different from that through which it blocks angiogenesis.

In this system, however, if fumagillin has an activity to arrest cell cycle at a phase other than G2 phase, an apparent reduction of G2 arrested cells would be observed. To examine this possibility, the effect of fumagillin on cell cycle progression was examined. After MT-Vpr1 cells were synchronized at G1/S border and released in the presence or absence of fumagillin, progression through S, G2, M and G1 was monitored by FACS analysis (Fig. 2B). In the absence of zinc, cell cycle progression was not affected by fumagillin (None and FM). When Vpr expression was induced by zinc addition, a similar fraction of cells was arrested at G2 at 12 h after the release regardless of the presence of fumagillin. But, in the presence of fumagillin, the fraction of cells arrested at G2 phase was significantly reduced at later time points (Zn and Zn + FM). These results indicate that fumagillin does not affect normal cell cycle progression but reduces the activity of Vpr to arrest the cell cycle. We have also confirmed that neither fumagillin nor TNP470 has any effect on the zinc induced Vpr expression level in MT-Vpr1 cells (Fig. 2C).

3.3. *Vpr inhibits growth of yeast cells independently from MetAP2 pathway*

Fumagillin is known to covalently bind and inhibit a protease, MetAP2 both in human and budding yeast cells [12,13]. However, since there are two reports contradicting each other about the matter whether inhibition of angiogenesis by fumagillin is dependent on the MetAP2 activity or not, the molecular mechanism through which fumagillin inhibits angiogenesis remains to be elucidated [14,15].

We examined whether MetAP2 is on the pathway for Vpr-dependent growth arrest and whether fumagillin blocks the activity of Vpr through the inhibition of MetAP2 or not. In budding yeast, the gene (*MAP2*) that encodes MetAP2 is not essential, because there is a second aminopeptidase, MetAP1, which is insensitive to fumagillin [12,13,18]. Vpr arrested the growth of Δ*map2* strain cells almost as completely as wild type, indicating that MetAP2 is not on the pathway of the Vpr dependent growth arrest (Fig. 3A). The ability of fumagillin to reverse the Vpr dependent arrest in Δ*map2* strain cells was confirmed on paper disk assay as well (data not shown). These results indicate that fumagillin abrogates Vpr function by targeting (a) molecule(s) other than MetAP2. Since the sensitivity to fumagillin and TNP470 is different for Vpr-dependent arrest and inhibition of angiogenesis, the target molecule(s) for these drugs may be different in these two systems.

3.4. *Mechanism of fumagillin to inhibit Vpr function*

Using biotinylated fumagillin, we attempted to detect any covalent or strong binding between Vpr and fumagillin. Biotinylated fumagillin was added to the lysates of MT-Vpr1 cells or yeast cells expressing FLAG-tagged Vpr. After the lysates were separated on SDS–PAGE and transferred on membrane, proteins covalently bound to fumagillin such as MetAP2 were probed with horse radish peroxidase (HRP) labelled streptavidin. Alternatively, proteins associated with biotinylated fumagillin were isolated using streptavidin conjugated agarose beads, and probed with αFLAG antibody to detect FLAG tagged Vpr. In spite of all of these attempts, we were unable to obtain any evidence for the interaction between Vpr and fumagillin (not shown). However, when point-mutations (Q3R, E25K, A30L, W54A, L64A, H71R, R73A, I74R, G75A, C76A, R80A, and R90K) were introduced into Vpr and their sensitivity to fumagillin was examined on paper disk assay, we found that the E25K mutation (the 25th glutamate of Vpr was changed to lysine) makes Vpr significantly resistant to fumagillin (Fig. 3B). Since the E25K Vpr still inhibits growth of yeast cells [25], the mechanism of fumagillin may

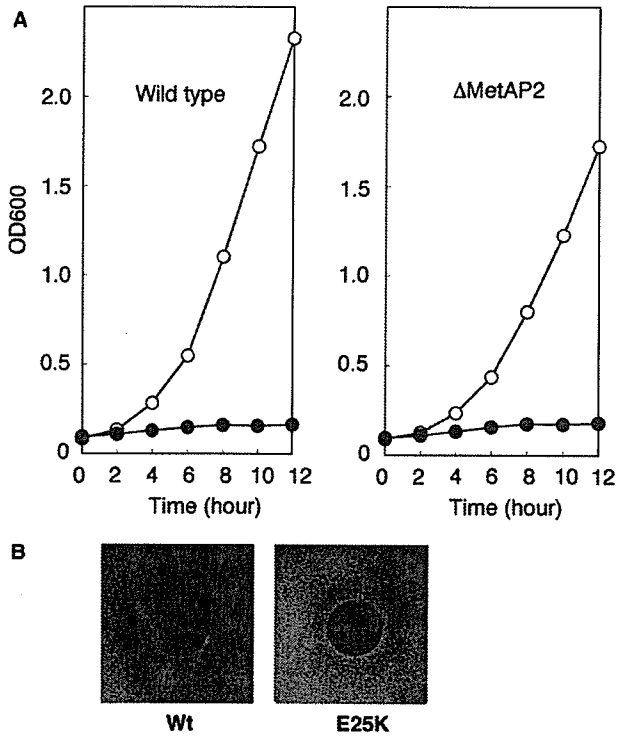

Fig. 3. Mechanism of fumagillin to abrogate the Vpr activity. (A) Vpr inhibits growth of yeast cells independently from MetAP2 activity. *Δmap2* cells (right) or its isogenic control cells (left) were cultured in the presence (closed circle) or absence (open circle) of the Vpr expression. The growth of yeast cells was monitored with the absorbance at 600 nm. (B) E25K mutation makes Vpr resistant to fumagillin. Yeast cells with wild type Vpr (left) or E25K mutated Vpr were embedded in agar plates as in Fig. 1. Paper filters with 20 μg of fumagillin were put on the plates and incubated for 3 days at 30 °C. Photographs were taken with translucent light to increase sensitivity.

be directly on Vpr rather than on a downstream pathway. The precise mechanism through which the E25K mutation renders Vpr resistant to fumagillin is not clear, but it is possible that fumagillin interacts directly (albeit too weakly to detect) with Vpr at residues surrounding E25.

3.5. Inhibition of Vpr-dependent viral gene expression by fumagillin or TNP470

Vpr is required for efficient replication of HIV-1 in non-dividing cells such as macrophages [2–4]. During the HIV-1 life cycle, Vpr functions after entry and reverse transcription, yet prior to, or at the time of, proviral transcription [2]. Thus we examined the effect of fumagillin on the proviral transcription upon the infection using an *env*-deficient HIV-1 vector that allows only a single round of infection. Wild type or frame-shifted Vpr-containing, *env*-deficient HIV-1 reporter vector in which Nef has been replaced by the luciferase gene (NL-Luc-R^+ or NL-Luc-R^-, respectively) [2] was used to infect primary human macrophages (Fig. 4A and B). Luciferase activity, determined 6 days after infection, was about 4 times higher from the Vpr^+ virus than that from the Vpr^- virus, indicating that Vpr is required for efficient expression of virally encoded genes in macrophages [2]. When fumagillin or TNP470 was added at the time of infection, luciferase expression from the Vpr^+ virus but not from the Vpr^- virus was inhibited in a dose-dependent manner. Under these experimental condition,

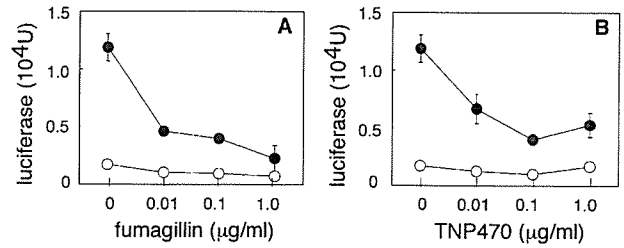

Fig. 4. Fumagillin and TNP470 inhibit Vpr dependent proviral gene expression. (A,B) Macrophages were infected with HIV-1 reporter vector with wild type (closed circle) or truncated (open circle) Vpr and cultured in the presence of fumagillin (A) or TNP470 (B). The proviral gene expression was monitored by the luciferase activity 6 days after the infection using luciferase assay substrate (Promega).

we could not see any sign of toxicity of 1 μg/ml of fumagillin for the macrophages under microscope indicating that the inhibition of viral gene expression in Vpr^+ infected cells is due to the inhibition of Vpr by these drugs rather than to some non-specific toxicity of them. Taken together, our results show that fumagillin or TNP470 suppresses the HIV-1 replication in macrophages through inhibition of Vpr-dependent viral gene expression.

3.6. Concluding remarks

Because it is now evident that Vpr's contribution to the pathogenesis of HIV-1 infection in vivo is crucial, Vpr has been proposed to be an attractive target for developing novel therapeutic strategies for AIDS therapy. Our results show that fumagillin and its derivatives can be used as a new type of AIDS therapeutic drug, which targets Vpr. In this context, it should be noted that fumagillin and TNP470 are already used clinically to treat Kaposi's sarcoma or microsporidiosis in AIDS patients with successful results [26,27], although the effects of these drugs on the viral replication have not been reported. Thus, the day when the fumagillin-derived compounds can be used clinically to prevent HIV-1 replication may come sooner than expected.

Acknowledgments: We thank T. Miyakawa, Y.-H. Chang and N.R. Landau for reagents; C. Tsutsui and A. Masumoto for assistance; members of RIKEN Antibiotics Laboratory for discussions; T. Hunter for critical reading of the manuscript; M. Watanabe and Y. Ikawa for encouragement. This work was supported in part by a Grant-in-Aid for Scientific Research on Priority Areas from the Ministry of Education, Culture, Sports, Science and Technology of Japan (MEXT) and by the Chemical Biology Research Project (RIKEN).

References

[1] Heinzinger, N.K., Bukinsky, M.I., Haggerty, S.A., Ragland, A.M., Kewalramani, V., Lee, M.A., Gendelman, H.E., Ratner, L., Stevenson, M. and Emerman, M. (1994) The Vpr protein of human immunodeficiency virus type 1 influences nuclear localization of viral nucleic acids in nondividing host cells. Proc. Natl. Acad. Sci. USA 91, 7311–7315.
[2] Connor, R.I., Chen, B.K., Choe, S. and Landau, N.R. (1995) Vpr is required for efficient replication of human immunodeficiency virus type-1 in mononuclear phagocytes. Virology 206, 935–944.
[3] Vodicka, M.A., Koepp, D.M., Silver, P.A. and Emerman, M. (1998) HIV-1 Vpr interacts with the nuclear transport pathway to promote macrophage infection. Genes Dev. 12, 175–185.
[4] Subbramanian, R.A., Kessous-Elbaz, A., Lodge, R., Forget, J., Yao, X.J., Bergeron, D. and Cohen, E.A. (1998) Human

immunodeficiency virus type 1 Vpr is a positive regulator of viral transcription and infectivity in primary human macrophages. J. Exp. Med. 187, 1103–1111.
[5] Andersen, J.L. and Planelles, V. (2005) The role of Vpr in HIV-1 pathogenesis. Curr. HIV Res. 3, 43–51.
[6] Le Rouzic, E. and Benichou, S. (2005) The Vpr protein from HIV-1: distinct roles along the viral life cycle. Retrovirology 2, 11.
[7] Muthumani, K., Choo, A.Y., Premkumar, A., Hwang, D.S., Thieu, K.P., Desai, B.M. and Weiner, D.B. (2005) Human immunodeficiency virus type 1 (HIV-1) Vpr-regulated cell death: insights into mechanism. Cell Death Differ. 12, 962–970.
[8] Goh, W.C., Rogel, M.E., Kinsey, C.M., Michael, S.F., Fultz, P.N., Nowak, M.A., Hahn, B.H. and Emerman, M. (1998) HIV-1 Vpr increases viral expression by manipulation of the cell cycle: a mechanism for selection of Vpr in vivo. Nat. Med. 4, 65–71.
[9] Somasundaran, M., Sharkey, M., Brichacek, B., Luzuriaga, K., Emerman, M., Sullivan, J.L. and Stevenson, M. (2002) Evidence for a cytopathogenicity determinant in HIV-1 Vpr. Proc. Natl. Acad. Sci. USA 99, 9503–9508.
[10] Lum, J.J., Cohen, O.J., Nie, Z., Weaver, J.G., Gomez, T.S., Yao, X.J., Lynch, D., Pilon, A.A., Hawley, N., Kim, J.E., Chen, Z., Montpetit, M., Sanchez-Dardon, J., Cohen, E.A. and Badley, A.D. (2003) Vpr R77Q is associated with long-term nonprogressive HIV infection and impaired induction of apoptosis. J. Clin. Invest. 111, 1547–1554.
[11] Ingber, D., Fujita, T., Kishimoto, S., Sudo, K., Kanamaru, T., Brem, H. and Folkman, J. (1990) Synthetic analogues of fumagillin that inhibit angiogenesis and suppress tumour growth. Nature 348, 555–557.
[12] Sin, N., Meng, L., Wang, M.Q., Wen, J.J., Bornmann, W.G. and Crews, C.M. (1997) The anti-angiogenic agent fumagillin covalently binds and inhibits the methionine aminopeptidase, MetAP-2. Proc. Natl. Acad. Sci. USA 94, 6099–6103.
[13] Griffith, E.C., Su, Z., Turk, B.E., Chen, S., Chang, Y.H., Wu, Z., Biemann, K. and Liu, J.O. (1997) Methionine aminopeptidase (type 2) is the common target for angiogenesis inhibitors AGM-1470 and ovalicin. Chem. Biol. 4, 461–471.
[14] Kim, S., LaMontagne, K., Sabio, M., Sharma, S., Versace, R.W., Yusuff, N. and Phillips, P.E. (2004) Depletion of methionine aminopeptidase 2 does not alter cell response to fumagillin or bengamides. Cancer Res. 64, 2984–2987.
[15] Bernier, S.G., Taghizadeh, N., Thompson, C.D., Westlin, W.F. and Hannig, G. (2005) Methionine aminopeptidases type I and type II are essential to control cell proliferation. J. Cell. Biochem. 95, 1191–1203.
[16] Watanabe, N., Yamaguchi, T., Akimoto, Y., Rattner, J.B., Hirano, H. and Nakauchi, H. (2000) Induction of M-phase arrest and apoptosis after HIV-1 Vpr expression through uncoupling of nuclear and centrosomal cycle in HeLa cells. Exp. Cell Res. 258, 261–269.
[17] Miyamoto, Y., Machida, K., Mizunuma, M., Emoto, Y., Sato, N., Miyahara, K., Hirata, D., Usui, T., Takahashi, H., Osada, H. and Miyakawa, T. (2002) Identification of *Saccharomyces cerevisiae* isoleucyl-tRNA synthetase as a target of the G1-specific inhibitor Reveromycin A. J. Biol. Chem. 277, 28810–28814.
[18] Li, X. and Chang, Y.H. (1995) Amino-terminal protein processing in *Saccharomyces cerevisiae* is an essential function that requires two distinct methionine aminopeptidases. Proc. Natl. Acad. Sci. USA 92, 12357–12361.
[19] Asami, Y., Kakeya, H., Onose, R., Chang, Y.-H., Toi, M. and Osada, H. (2004) RK-805, an endothelial-cell-growth inhibitor produced by *Neosartorya* sp. and a docking model with methionine aminopeptidase-2. Tetrahedron 60, 7085–7091.
[20] Marui, S., Itoh, F., Kozai, Y., Sudo, K. and Kishimoto, S. (1992) Chemical modification of fumagillin. I. 6-*O*-acyl, 6-*O*-sulfonyl, 6-*O*-alkyl, and 6-*O*-(*N*-substituted-carbamoyl)fumagillols. Chem. Pharm. Bull. (Tokyo) 40, 96–101.
[21] Cheng-Mayer, C., Quiroga, M., Tung, J.W., Dina, D. and Levy, J.A. (1990) Viral determinants of human immunodeficiency virus type 1 T-cell or macrophage tropism, cytopathogenicity, and CD4 antigen modulation. J. Virol. 64, 4390–4398.
[22] Macreadie, I.G., Castelli, L.A., Hewish, D.R., Kirkpatrick, A., Ward, A.C. and Azad, A.A. (1995) A domain of human immunodeficiency virus type 1 Vpr containing repeated H(S/F)RIG amino acid motifs causes cell growth arrest and structural defects. Proc. Natl. Acad. Sci. USA 92, 2770–2774.
[23] Jowett, J.B., Planelles, V., Poon, B., Shah, N.P., Chen, M.L. and Chen, I.S. (1995) The human immunodeficiency virus type 1 vpr gene arrests infected T cells in the G2 + M phase of the cell cycle. J. Virol. 69, 6304–6313.
[24] He, J., Choe, S., Walker, R., Di Marzio, P., Morgan, D.O. and Landau, N.R. (1995) Human immunodeficiency virus type 1 viral protein R (Vpr) arrests cells in the G2 phase of the cell cycle by inhibiting p34cdc2 activity. J. Virol. 69, 6705–6711.
[25] Yao, X.J., Rougeau, N., Duisit, G., Lemay, J. and Cohen, E.A. (2004) Analysis of HIV-1 Vpr determinants responsible for cell growth arrest in *Saccharomyces cerevisiae*. Retrovirology 1, 21.
[26] Dezube, B.J., Von Roenn, J.H., Holden-Wiltse, J., Cheung, T.W., Remick, S.C., Cooley, T.P., Moore, J., Sommadossi, J.P., Shriver, S.L., Suckow, C.W. and Gill, P.S. (1998) Fumagillin analog in the treatment of Kaposi's sarcoma: a phase I AIDS Clinical Trial Group study. AIDS Clinical Trial Group No. 215 Team. J. Clin. Oncol. 16, 1444–1449.
[27] Didier, E.S. (2005) Microsporidiosis: an emerging and opportunistic infection in humans and animals. Acta Trop. 94, 61–76.

Resistance profile of a neutralizing anti-HIV monoclonal antibody, KD-247, that shows favourable synergism with anti-CCR5 inhibitors

Kazuhisa Yoshimura[a], Junji Shibata[a], Tetsuya Kimura[a], Akiko Honda[a], Yosuke Maeda[b], Atsushi Koito[a], Toshio Murakami[c], Hiroaki Mitsuya[d] and Shuzo Matsushita[a]

Background: The high-affinity humanized monoclonal antibody (MAb) KD-247 reacts with a tip region in gp120-V3 and cross-neutralizes primary isolates with a matching neutralization sequence motif.

Methods: We induced an HIV-1 variant that was resistant to KD-247 by exposing the JR-FL virus to increasing concentrations of KD-247 in PM1/CCR5 cells, which expressed high levels of CCR5 *in vitro*. We determined the amino acid sequence of the gp120-encoding region of the JR-FL escape mutant from KD-247. To confirm that this substitution was responsible for the KD-247-resistance, a single-round replication assay was performed. We further evaluated the anti-HIV-1 interactions between KD-247 and various CCR5 inhibitors *in vitro*.

Results: At passage 8 of the culture in the presence of 1000 μg/ml KD-247, one amino acid substitution, Gly to Glu at position 314 (G314E), was identified in the V3-tip of gp120. A pseudotyped virus with the G314E mutation was highly resistant to KD-247. Unexpectedly, this mutant virus was sensitive to CCR5 inhibitors, RANTES, recombinant human soluble CD4 (rsCD4) and an anti-CCR5 MAb, but resistant to an anti-CD4 MAb, compared with the wild-type virus. We also found that combinations of KD-247 and CCR5 inhibitors were highly synergistic.

Conclusions: The present data suggest that KD-247 has certain advantages for possible passive immunotherapy. They are: high concentrations of KD-247 are needed for viral acquisition of KD-247 resistance; the escape variants are more sensitive to CCR5 inhibitors and rsCD4; and there are high levels of synergism between KD-247 and CCR5 inhibitors at all concentrations tested.

AIDS 2006, **20**:2065–2073

Keywords: HIV-1, KD-247, anti-V3 monoclonal antibody, broadly neutralizing, CCR5 inhibitor, synergism

From the [a]Division of Clinical Retrovirology and Infectious Diseases, Center for AIDS Research, Graduate School of Medical Sciences, Kumamoto University, Kumamoto, Japan, the [b]Department of Medical Virology, Graduate School of Medical Sciences, Kumamoto University, Kumamoto, Japan, the [c]The Chemo-Sero-Therapeutic Research Institute, Kyokushi, Kikuchi, Kumamoto, Japan, and the [d]Department of Internal Medicine II, Graduate School of Medical Sciences, Kumamoto University, Kumamoto, Japan.

Correspondence to S. Matsushita, Division of Clinical Retrovirology and Infectious Diseases, Center for AIDS Research, Kumamoto University, Kumamoto 860-0811, Japan.

Tel: +81 96 373 6536; fax: +81 96 373 6537; e-mail: shuzo@kaiju.medic.kumamoto-u.ac.jp

These data were presented at the *Thirteenth Conference on Retroviruses and Opportunistic Infections*. Denver, CO, February 2006 [abstract 506].

Note: K. Yoshimura and J. Shibata contributed equally to this work.

Received: 21 February 2006; accepted: 27 July 2006.

ISSN 0269-9370 © 2006 Lippincott Williams & Wilkins

Introduction

In a recent paper, we described a cross-neutralizing anti-V3 antibody, KD-247, against primary isolates via sequential immunization with six peptides from V3 that contained a neutralizing epitope of HIV-1 [1]. The ability of KD-247 to neutralize HIV-1 may be dependent on site-specific binding to an epitope on the viral envelope glycoprotein. The complementarity determining regions of KD-247 were transferred from the mouse monoclonal antibody (MAb) C25, which was designed to have broad neutralization activity against HIV-1 clade B isolates. The recognition site of KD-247 was mapped to five or six amino acids around the PGR core sequence at the tip of the V3 region of gp120. The shortest reactive peptide recognized by KD-247 was determined to be IGPGR, although the epitope was stabilized by the addition of one or more supplemental amino acids. The GPGR sequence in the V3 tip is highly conserved among HIV-1 strains [2]. In a recent study, we showed that the reshaped MAb KD-247 was suitable for use not only as an antibody for passive immunization for the prevention of HIV infection but also as an antibody for passive transfer immunotherapy for infected individuals [3].

In the present study, we induced HIV-1 variants that escaped from neutralization by KD-247 *in vitro* by continuously exposing the R5 virus JR-FL to increasing concentrations of KD-247 and defined the virological properties of a pseudotyped HIV-1 clone carrying the KD-247 escape-associated *env* gene mutation. We also evaluated the anti-HIV-1 interactions between KD-247 and various CCR5 inhibitors *in vitro*.

Materials and methods

Cells, culture conditions and reagents

The CD4-positive T-cell line PM1 was maintained in RPMI 1640 (Sigma, St. Louis, Missouri, USA) supplemented with 10% heat-inactivated foetal calf serum (Hyclone, Logan Utah, USA), 50 U/ml penicillin and 50 μg/ml streptomycin. PM1/CCR5 cells were generated by standard retrovirus-mediated transduction of PM1 cells with pBABE-CCR5 provided by the National Institutes of Health AIDS Research and Preference Reagent Program [4]. PM1 and PM1/CCR5 cells were analysed for their surface expressions of CD4, CCR5 and CXCR4 using a FACSCalibur (Becton Dickinson, Franklin Lakes, New Jersey, USA). 293T cells were maintained in Dulbecco's modified Eagle medium (DMEM; Sigma) supplemented with 10% heat-inactivated FCS. The CD4 human osteogenic sarcoma cell line GHOST was maintained in DMEM supplemented with 10% FCS, 200 μg/ml G418 (Gibco BRL, Rockville, Maryland, USA) and 100 μg/ml hygromycin B (Sigma). The GHOST derivatives GHOST-hi5 and GHOST-CXCR4 stably expressed CCR5 and CXCR4, respectively, as described elsewhere [5], and were selected with 1 μg/ml puromycin (Sigma).

17b, a CD4-induced (CD4i) MAb, was a kind gift from J. Robinson (Department of Pediatrics, Tulane University Medical Center, New Orleans, Louisiana, USA). 447-52D, an anti-gp120 V3 MAb, was a kind gift from S. Zolla-Pazner (Department of Pathology, New York University School of Medicine, New York, USA). 2D7, an anti-CCR5 MAb, and RPA-T4, an anti-CD4 MAb, were purchased from BD Biosciences Pharmingen (San Jose, California, USA). 2′,3′-dideoxyinosine (ddI, didanosine) was from Calbiochem, San Diego, California, USA. 3′-thiacytidine (3TC, lamivudine) was a kind gift from R. F. Schinazi (Department of Pediatrics, Emory University School of Medicine, Atlanta, Georgia, USA). Saquinavir (SQV) was kindly provided by Roche Products Ltd., Welwyn Garden City, UK. Amprenavir (APV) was a kind gift from GlaxoSmithKline, Middlesex, UK. Nelfinavir (NFV) and indinavir (IDV) were kindly provided by Japan Energy Inc., Tokyo, Japan. Recombinant human soluble CD4 (rsCD4), MIP-1α, MIP-1β and RANTES were from R&D Systems Inc., Abingdon, UK. The CCR5 inhibitors TAK-779 [6] and SCH-351125 (SCH-C) [7] were synthesized as previously described. AK-602, a CCR5 inhibitor, was kindly provided by Ono Pharmaceutical Co. Ltd., Osaka, Japan [8].

Isolation of a KD-247-resistant mutant from JR-FL *in vitro*

For the selection of a KD-247 escape virus, JR-FL [9] was treated with various concentrations of KD-247 and then infected into PM1/CCR5 cells as previously described with minor modifications [10]. Viral replication was monitored by observation of any cytopathic effects in PM1/CCR5 cells. The culture supernatant was harvested on day 7 and used to infect fresh PM1/CCR5 cells for the next round of culture in the presence of increasing concentrations of KD-247. After the virus was passaged in the presence of up to 1000 μg/ml KD-247 in PM1/CCR5 cells, a KD-247-resistant virus, JR-FL(1000)8P, was recovered from the cell culture supernatant. JR-FL was also passaged for the same time periods in PM1/CCR5 cells in the absence of KD-247 to exclude any effects of the long-term culture of eight passages, and the resulting virus was designated JR-FL(−)8P.

The sensitivities of the passage 8 JR-FL viruses in the presence or absence of KD-247 to various drugs or MAb were determined as previously described with minor modifications [11]. Briefly, PM1-CCR5 cells (2×10^3/well) were exposed to 100 50% tissue culture inhibitory doses ($TCID_{50}$) of the JR-FL(1000)P8 or JR-FL(−)P8 in the presence of various concentrations of drugs or MAb in 96-well round-bottom plates. The 50% inhibitory concentration (IC_{50}) values were determined using the MTT {3-(4,5-Dimethylthiazol-2-yl)-2,5-diphenyltetrazolium

bromide} (MTT) assay on day 7 of culture. All assays were performed in duplicate.

Viral RNA (0.5 μg) extracts from cell culture supernatants at several concentrations of KD-247 were reverse-transcribed using a High Capacity cDNA Archive Kit (Applied Biosystems, Foster City, California, USA). The cDNA obtained were subjected to PCR amplification using *Taq* polymerase. After cloning the amplified products into pCR2.1, the Env regions in both the passaged and selected viruses were sequenced using an ABI PRISM 310 automated DNA sequencer (Applied Biosystems).

Construction of mutant envelope expression vectors and production of pseudovirions

For the construction of mutant envelope expression vectors, we used pCXN2, which contains a chicken actin promoter. Briefly, the JR-FL *env* region was cloned by PCR and ligated into pCR2.1, generating pCR2-FL_{wt}. The *Eco*RI fragment of pCR2-FL_{wt} containing the entire *env* region was ligated into pCXN2 to give pCXN-FL_{wt} [9]. A mutant Env (G314E) expression vector was generated from pCXN-FL_{wt} using a QuikChange site-directed mutagenesis kit (Stratagene, Chedar Creek, Texas, USA) and the primers JR-FLv3G/Efw (5′–TACATA-TAGGACCAGAGAGAGCATTTTATAC–3′) and JR-FLv3G/Erv (5′–GTATAAAATGCTCTCTCTGGTCC TATATGTA–3′) according to the manufacturer's protocol, and designated pCXN-FLG314E.

Plasmids pNL4-3.Luc.R^-E^- and pRSV-Rev [12], supplied by the NIH AIDS Research and Reference Reagent Program, and plasmid pCXN2, expressing wild-type or G314E Env, were cotransfected into 293T cells using the Effectene Transfection Reagent (Qiagen, Valencia, California, USA). At 24 h after the transfection, the pseudovirus-containing supernatants were harvested, filtered through a 0.2-μm pore-size filter and stored at −150°C. For measurement of the pseudovirus activities, a luminescence assay with GHOST-hi5 cells was used as previously described [13].

Neutralization assays

A single-cycle infectivity assay was used to measure the neutralization of JR-FL_{wt} or JR-FL_{GPER} pseudovirions as described previously [13]. Briefly, MAb at various concentrations and a pseudovirus suspension corresponding to 200 $TCID_{50}$ were preincubated for 15 min on ice. The virus–antibody mixtures were added to GHOST-hi5 cells, which had been seeded in a 96-well plate (1.5×10^4 cells/well) on the previous day. The cultures were incubated for 2 days at 37°C, washed with phosphate-buffered saline and lysed with lysis buffer (Luc PGC-50; PicaGene, Tokyo, Japan). Following transfer of the cell lysates to luminometer plates (Costar 3912), the luciferase activity (in relative light units) in each well was measured using Luciferase Substrate (100 μl/well; PicaGene) in a TR717 microplate luminometer (Applied Biosystems). The reduction in infectivity was determined by comparing the relative light units in the presence and absence of MAb and expressed as the percent neutralization. The same assay was repeated two to three times.

In vitro binding assay to the JR-FL_{wt} or JR-FL_{GPER} envelope

The JR-FL gp160 coding sequence was amplified from the infectious clone vector (pJR-FL) using the primers ENVA-*Eco*RI (5′–CGGAATTCGGCTTAGGCATCT CCTATGGCAGGAAGAA–3′) and ENVN-*Bam*HI (5′–CGGGATCCCGCTGCCAATCAGGGAAGTAG CCTTGTGT–3′). The product was digested with *Eco*RI and *Bam*HI and subcloned into the corresponding sites in pDNR-1r (Clontech) for sequencing and subsequent manipulation. A JR-FL_{GPER} Env expression vector was generated from pDNR-JR-FL_{wt} using a QuikChange site-directed mutagenesis kit and the primers JR-FLv3G/Efw and JR-FLv3G/Erv according to the manufacturer's protocol. The wild-type and mutated *env* gene fragments were then subcloned into pLP-IRES2-EGFP (Clontech) using Cre-recombinase (Clontech) according to the manufacturer's instructions, and designated pLP-EGFP-JR-FL_{wt} and pLP-EGFP-JR-FL_{GPER}, respectively.

293T cells were cotransfected with pRSV-Rev (0.5 μg) and pLP-IRES2-EGFP, pLP-EGFP-JR-FL_{wt} or pLP-EGFP-JR-FL_{GPER} (9.5 μg) using the Effectene Transfection Reagent (Qiagen). After 36 h, the cells were harvested, incubated with each anti-HIV-1 MAb with or without rsCD4 (0.5 μg/ml) in combination with biotin-conjugated anti-human IgG and peridinin chlorophyll-a protein-conjugated streptavidin (BD Biosciences Pharmingen), gated for the GFP-positive area and analysed using a FACSCalibur.

Data analysis and evaluation of synergy

Analysis of the synergistic, additive or antagonist effects of the antiviral agents was first performed according to the median effect principle using the CalcuSyn version 2 computer program [14,15] to provide estimates of the IC_{50} values of the antiviral reagents in different combinations. Combination indices (CI) were estimated from the data and reflected the nature of the interactions between KD-247 and the CCR5 inhibitors against JR-FL(−)8P in PM1/CCR5 cells, as evaluated using the MTT assay. Specifically, $CI < 0.9$ indicated synergy, $0.9 < CI < 1.1$ indicated additivity and $CI > 1.1$ indicated antagonism. The value of CI was directly proportional to the amount of synergy in the combination regimen. For example, values of $CI < 0.5$ represented a high degree of synergy, whereas values of $CI > 1.5$ represented significant antagonism. This approach has been widely used in analyses of antiviral interactions and was chosen to allow comparability with published literature.

Statistical analysis

Statistical correlations were analysed using Student's t test. P values < 0.05 were considered statistically significant.

Results

Selection of a KD-247 escape variant

For the isolation of a KD-247 escape mutant from R5 HIV *in vitro*, PM1 cells expressing high levels of CCR5, designated PM1/CCR5 cells, which were highly sensitive to both X4 and R5 HIV infection and accompanied by prominent syncytia [4] were used as the target cells. An R5 HIV strain, JR-FL, which uses CCR5 as its coreceptor was used for the selection of a KD-247 escape virus.

In order to select an HIV-1 variant that can escape from neutralization by KD-247 *in vitro*, we exposed PM1/CCR5 cells to JR-FL, and serially passaged the virus in the presence of increasing concentrations of KD-247, or in the absence of the MAb as a control. The selected virus was initially propagated in the presence of 1 μg/ml KD-247, and during the course of the selection procedure, the MAb concentration was increased to 1000 μg/ml. At passage 8, the supernatants containing the passaged viruses in the presence or absence of KD-247, designated JR-FL(1000)8P and JR-FL(−)8P, respectively, were harvested and titrated for their infectivities and sensitivities to KD-247, CCR5 inhibitors (TAK-779, SCH-C and AK-602), nucleoside reverse transcriptase inhibitors (NRTI; ddI and 3TC) and protease inhibitors (PI; NFV, IDV, APV and SQV), as evaluated by the MTT assay (Table 1). The IC_{50} values of KD-247 against JR-FL(−)8P and JR-FL(1000)8P were 6.3 and > 100 μg/ml, respectively. The fold difference between these IC_{50} values was > 16. JR-FL(1000)8P was sensitive to all the NRTI and PI, similar to JR-FL(−)8P. Unexpectedly, JR-FL(1000)8P was more sensitive to the three CCR5 inhibitors (TAK-779, SCH-C and AK-602), rsCD4, anti-CCR5 MAb 2D7 and RANTES than JR-FL(−)8P. However, JR-FL(1000)8P was threefold more resistant to anti-CD4 MAb RPA-T4 than JR-FL(−)8P. These data suggest that the escape variant with a highly resistant phenotype against KD-247 becomes more sensitive to CCR5 inhibitors and rsCD4, and needs higher concentration of anti-CD4 antibody for entry blocking, compared with JR-FL(−)8P.

Sequencing of the envelope region of the KD-247 escape mutant

To determine the region responsible for the reduced sensitivity of the escape mutant to KD-247, the C1–C4 regions of the envelope were sequenced after cloning of the PCR product of each region using cDNA synthesized from viral RNA obtained from the supernatants of infected cells as templates. A total of 12–16 clones for each PCR product were isolated and sequenced. Analyses of the *env* sequences of these products revealed that the selected virus had a Gly→Glu substitution at codon 314 (G314E) in the V3 region of the envelope at passage 7 (600 μg/ml; 10/12 clones) and passage 8 (1000 μg/ml; 12/16 clones) (Fig. 1). Some changes in the envelope sequence in other regions, including C1, V1, V2, C2, C3, V4 and C4 of the escape mutant were found as well as in V3 around the IGPGR sequence even at early time points in the presence of the selective pressure. It is possible that these mutations also confer resistance to KD-247 but lead to virus of decreased fitness and thus they did not expand in a next passage except for the G314E. On the other hand, the virus passaged in PM1/CCR5 cells

Table 1. Anti-HIV-1 activities of various MAb and inhibitors toward KD247-resistant JR-FL.

Antibody or inhibitor	$IC_{50} \pm SD$[a]		Fold change	P[b]
	JR-FL(−)8P	JR-FL(1000)8P		
KD-247 (μg/ml)	6.3 ± 5.0	> 100	< 16	**< 0.01**
TAK-779 (nM)	217 ± 50.3	54.7 ± 29.5	0.3	**< 0.01**
SCH-C (nM)	27.5 ± 3.5	8.0 ± 1.4	0.3	**0.02**
AK-602 (nM)	7.1 ± 4.5	0.15 ± 0.08	0.02	**0.02**
Didanosine (μM)	1.0 ± 0.57	1.0 ± 0.27	1.0	0.98
Lamivudine (μM)	0.33 ± 0.01	0.29 ± 0.04	0.9	0.30
Nelfinavir (μM)	0.033 ± 0.001	0.036 ± 0.006	1.1	0.56
Indinavir (μM)	0.017 ± 0.004	0.016 ± 0.005	0.9	0.85
Amprenavir (μM)	0.022 ± 0.001	0.017 ± 0.008	0.8	0.47
Saquinavir (μM)	0.0038 ± 0.0004	0.0034 ± 0.0004	0.9	0.42
rsCD4 (μg/ml)	3.3 ± 0.07	0.57 ± 0.48	0.2	**0.02**
Anti-CD4 MAb (RPA-T4) (μg/ml)	0.01 ± 0.004	0.03 ± 0.004	3.0	**0.01**
Anti-CCR5 MAb (2D7) (μg/ml)	0.19 ± 0.03	0.066 ± 0.005	0.3	**0.03**
MIP-1α (μg/ml)	0.006 ± 0.002	0.0029 ± 0.001	0.5	0.11
MIP-1β (μg/ml)	0.39 ± 0.08	0.23 ± 0.18	0.6	0.22
RANTES (μg/ml)	0.045 ± 0.0007	0.005 ± 0.001	0.1	**0.02**

[a]PM1/CCR5 cells (2×10^3) were exposed to 100 TCID50 of JR-FL(−)8P or JR-FL(1000)8P and then cultured in the presence of various concentrations of MAb or inhibitors. The IC_{50} values were determined using the MTT assay on day 7 of culture. Data shown represent values derived from the results of two or three independent experiments conducted in duplicate.
[b]P values < 0.05 were considered statistically significant (shown in bold type). IC, Inhibitory concentration.

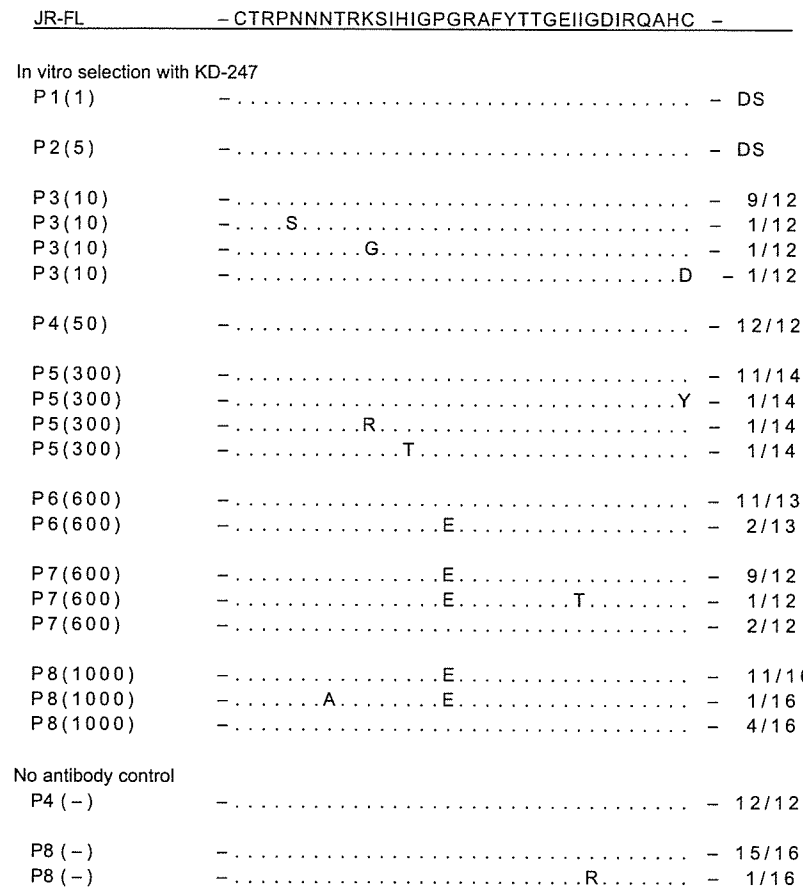

Fig. 1. V3 amino acid sequences from the supernatants of JR-FL-infected PM1/CCR5 cells passaged in the presence or absence of KD-247. Viral RNA from the cell culture supernatants at several concentrations of KD-247 was reverse-transcribed. After subjecting the obtained cDNA to PCR amplification and cloning, the *env* regions in the viruses passaged in the presence or absence of KD-247 were sequenced. The wild-type JR-FL amino acid sequence of V3 is shown at the top. The numbers on the right show the numbers of clones with the listed sequence among the total number of clones tested. In each set of clones, the deduced amino acid sequence of the V3 region was aligned by the single amino acid code. Dots denote sequence identity. DS, Direct sequence.

without KD-247 did not show the G314E substitution at either passage 4 (0/12 clones) or passage 8 (0/16 clones) (Fig. 1).

Susceptibilities of HIV-1 containing the KD-247-associated G314E substitution to MAb and drugs

To confirm whether the G314E mutation was responsible for the reduced sensitivity to KD-247, a single-round replication assay was performed. Luciferase-reporter viruses were pseudotyped with wild-type JR-FL (JR-FL_{wt}) or singly mutated with G314E (JR-FL_{G314E}) in the V3 region. As shown in Fig. 2a, JR-FL_{G314E} was completely resistant to KD-247 up to 100 μg/ml. We also examined the sensitivities of the pseudotyped clones to rsCD4, anti-CD4 MAb RPA-T4 and anti-CCR5 MAb 2D7 by a single-round replication assay (Fig. 2b–d). As expected, JR-FL_{G314E} was more sensitive to rsCD4 and 2D7, but fourfold more resistant to RPA-T4, compared to JR-FLwt, similar to the results for the passaged viruses with or without KD-247.

Next, we determined the sensitivities of JR-FL_{G314E} to three CCR5 inhibitors (TAK-779, SCH-C and AK-602). The IC_{50} values of TAK-779, SCH-C and AK-602 against JR-FL_{G314E} were 20-, 10- and 5-fold lower than the corresponding values against JR-FL_{wt}, respectively (Fig. 2e–g). These results confirmed that the G314E mutation was associated with the observed reduction in the sensitivities of JR-FL(1000)8P to KD-247 and RPA-T4, and also with the increased sensitivities to rsCD4, 2D7 and CCR5 inhibitors.

Next, we analysed the sensitivities of JR-FL_{wt} and JR-FL_{G314E} to another broad-specificity neutralizing anti-V3 MAb 447-52D and the CD4i MAb 17b (Fig. 2h and i). Interestingly, JR-FL_{G314E} was more sensitive to both 17b (< 0.8-fold change in the IC_{50}) and 447-52D (0.1-fold change in the IC_{50}) than JR-FLwt (Fig. 2h and i). A similar result regarding neutralization sensitivity to 17b was reported when viruses were pretreated with rsCD4 [16]. In our result, JR-FL_{G314E} was more sensitive to 17b

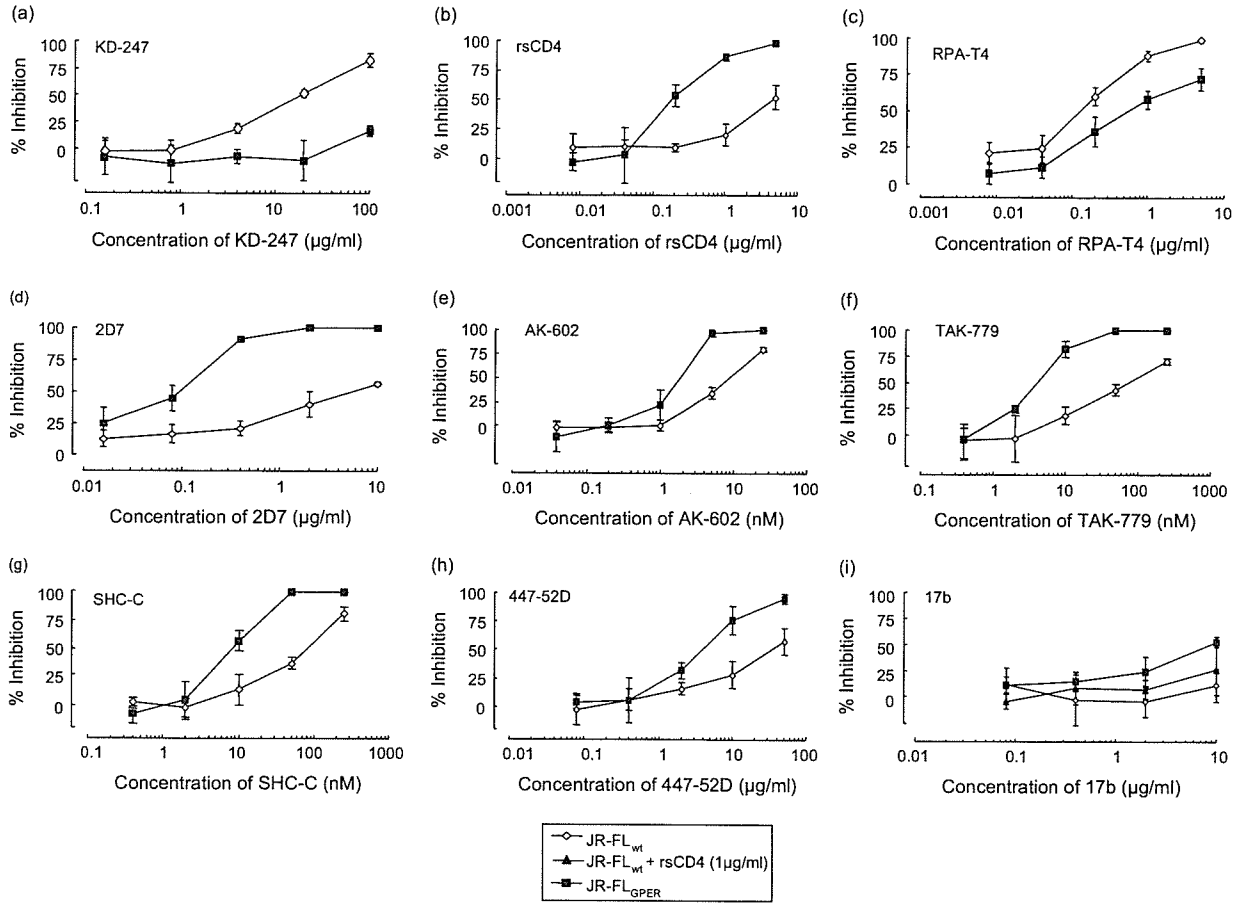

Fig. 2. Sensitivities of luciferase reporter HIV strains pseudotyped with the G314E envelope mutation to MAb, rsCD4 and CCR5 inhibitors. KD-247 (a), rsCD4 (b), 447-52D (h) and 17b with or without rsCD4 (1 μg/ml) (i) were preincubated with luciferase reporter HIVs pseudotyped with wild-type JR-FL (JR-FL$_{wt}$) or the G314E envelope mutant (JR-FL$_{GPER}$) for 15 min, followed by addition of the mixtures to the target cells (GOHST-hi5). The target cells were treated with RPA-T4 (c), 2D7 (d), AK-602 (e), TAK-779 (f) and SCH-C (g) for 15 min, followed by an inoculation of the pseudotype clones. Inhibitory effects were determined by measuring the luciferase activities on day 2 of culture.

than JR-FLwt preincubated with rsCD4 (1 μg/ml) (Fig. 2i).

Comparison of antibody binding to cell surface-expressed wild-type and GPER mutant Env

To elucidate the mechanism of the increased sensitivities of the escape virus with the G314E mutation in the V3-tip to 17b and 447-52D, wild-type or mutant Env-expressing 293T cells were established by transfecting each Env expression plasmid, and then stained with the MAb in the presence or absence of rsCD4 (0.5 μg/ml). Binding of a patient's IgG, KD-247, 17b or 447-52D to the surface-expressed Env proteins was assayed using a fluorescence-activated cell sorter analysis. As shown in Fig. 3, KD-247 bound to the wild-type JR-FL Env, but not the GPER mutant Env, while the other anti-V3 MAb, 447-52D, bound to both the Env proteins very well, especially the mutant Env. The mean fluorescence intensity (MFI) of 447-52D increased from 87.56 (wild-type Env) to 219.47 (GPER Env). Without rsCD4, the CD4i 17b MAb bound slightly to the wild-type Env (MFI, 33.21; Fig. 3) but failed to neutralize JR-FL$_{wt}$ (Fig. 2i). On the other hand, in the presence of rsCD4 (0.5 μg/ml), a shift in the MFI was observed with 17b binding to the surface of wild type-Env-expressing cells. In contrast to these data for wild-type Env, 17b bound to the mutant Env efficiently in the absence of rsCD4 at a higher level than to the wild-type Env in the presence of rsCD4 (MFI, 97.33 for the mutant Env versus 56.61 for the wild-type Env; Fig. 3). 17b was also able to neutralize JR-FL$_{GPER}$, even in the absence of rsCD4 (Fig. 2i). These results suggest that the G314E mutation in the V3-tip induces the expression of cryptic epitopes for antibodies against the CD4i epitope and V3 loop, such that the mutant virus is neutralized by the CD4i MAb without rsCD4 or by lower concentrations of the anti-V3 MAb compared with the wild-type virus.

Highly synergistic interactions of KD-247 combined with CCR5 inhibitors

Both neutralizing MAb and chemokine receptor inhibitors attack the viral entry process, especially at the stage of the chemokine receptor-gp120 (V3)

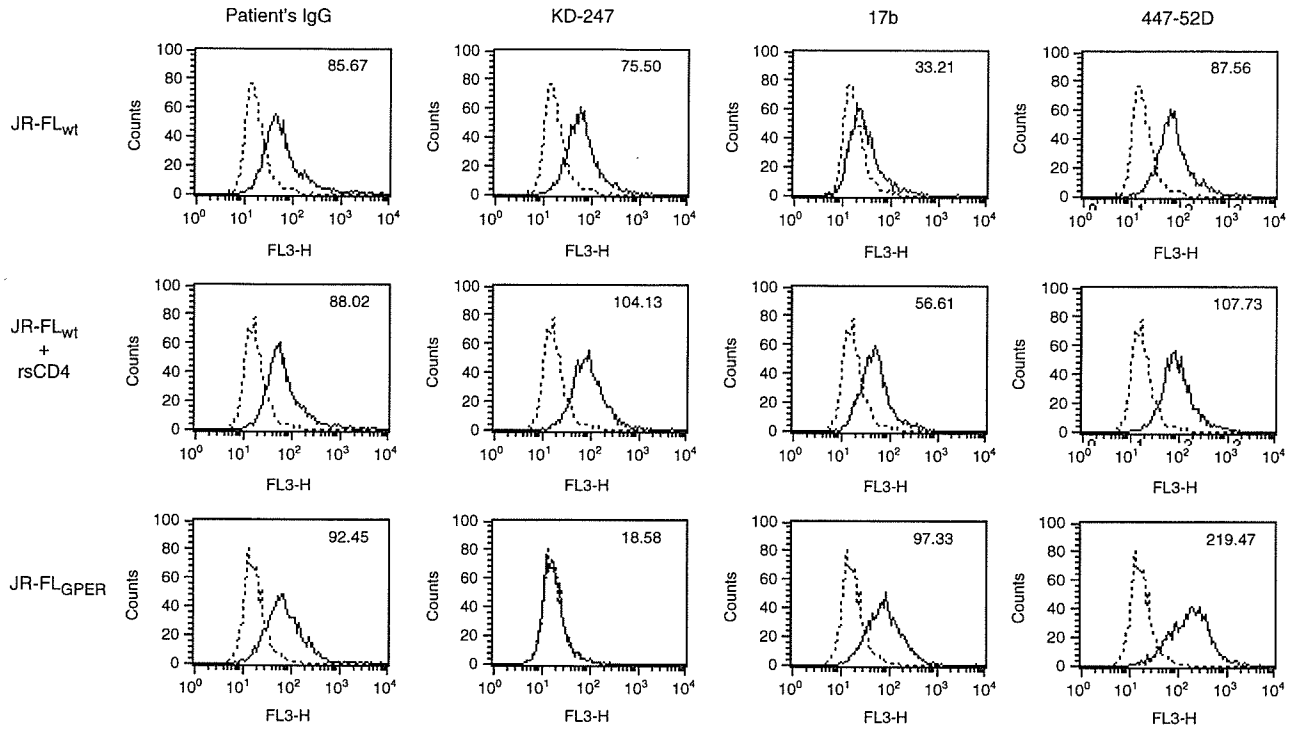

Fig. 3. Comparison of antibody binding to cell surface-expressed wild-type and GPER mutant Envs. 293T cells transfected with wild-type and GPER mutant Env-expression vectors were harvested at 36 h post-transfection and stained with the indicated antibodies. Flow cytometry data for binding of the indicated antibodies (black lines) to cell surface wild-type Env (upper), wild-type Env in the presence of 0.5 μg/ml of rsCD4 (middle) and GPER mutant Env (lower) are shown among GFP-gated 293T cells along with a control antibody (anti-human CD19; dotted lines). Data are representative of the results from at least two independent experiments. The number at the top right of each graph shows the MFI of the indicated antibodies.

interaction. Each of them binds to either CCR5 or gp120. Furthermore, our present observations suggest that the neutralizing MAb KD-247 selects an escape variant with greater sensitivity to chemokine receptor inhibitors. Based on this notion, we attempted to test the synergy of this MAb with chemokine receptor inhibitors against wild-type JR-FL.

The multiple-drug-effect analysis of Chou and colleagues [14,15] was used to analyse the effects of combinations of KD-247 with CCR5 inhibitors against JR-FL(−)8P in PM1/CCR5 cells (Table 2). As shown in Table 2, all the CI values for KD-247 with the CCR5 inhibitors (TAK-779, AK-602 or SCH-C) were < 0.5 against JR-FL(−)8P at all the inhibitory concentrations tested. In particular, the CI values for the combinations of KD-247 with SCH-C and AK-602 were less than 0.1 for IC_{90}. These results suggest that combination of KD-247 with any of the tested CCR5 inhibitors produces very highly synergistic interactions at not only high but also low inhibitory concentrations. We further evaluated the *in vitro* interactions between KD-247 and representatives of each class of currently available antiretroviral agents. Although KD-247 had favourable drug interactions with all of the agents (data not shown), the synergistic effects of KD-247 and CCR5 inhibitors were the most potent among all the combinations tested in this study.

Table 2. Combination indices (CI) for KD-247 and CCR5 inhibitors against virus JR-FL(−)8P.

CCR5 inhibitor used in combination with KD-247 (2.5–160 μg/ml)	CI values at different IC[a]		
	IC_{50}	IC_{75}	IC_{90}
AK-602 (0.3–20 nM)	0.21	0.12	0.07
TAK-779 (12.5–800 nM)	0.23	0.19	0.16
SCH-C (3–100 nM)	0.18	0.08	0.04

[a]The multiple-drug-effect analysis of Chou and colleagues was used to analyse the effects of the drugs in combination [15]. IC, Inhibitory concentration. CI < 1, synergy; 0.9 < CI < 1.1, additivity; CI > 1.1, antagonism.

Discussion

Although KD-247 shows clinical promise as a passive immunization agent for suppressing viral spread in phenotype-matched HIV-infected individuals, we also know that HIV-1 always escapes from the selection pressure of any one inhibitor by obtaining mutation(s). Therefore, we induced an HIV-1 variant that could escape from neutralization by KD-247 *in vitro* by continuously exposing the R5 virus JR-FL to increasing concentrations of KD-247 and defined the virological

properties and susceptibilities of this variant to other monoclonal antibodies (CD4i, anti-V3, anti-CD4 and anti-CCR5 MAb). The present data suggest that the KD-247 escape variant, which has a G314E mutation in the V3-tip, has not only a highly resistant phenotype against KD-247 but also greater sensitivities to CCR5 inhibitors and rsCD4, and needs higher concentration of anti-CD4 antibody for entry blocking compared with the corresponding control virus after eight passages in the absence of KD-247. These phenomena were confirmed using a pseudotyped virus containing the KD-247 escape-related G314E mutation by a single-round neutralizing assay. No previous studies have reported this G314E mutation in the V3-tip region of the R5 virus using in vitro selection by MAb. This mutation is also very rare in clinical isolates from HIV-1-infected patients [17]. Interestingly, this mutation in the V3-tip also influences the sensitivities to CCR5 inhibitors, rsCD4, anti-CD4 MAb and CD4i MAb 17b. It is not clear why KD-247 escape mutant became sensitive to rsCD4 and CCR5 inhibitors. It is conceivable that higher expression of CCR5 and CD4 on PM1/CCR5 cells may have some effect on the selection of such phenotype.

The ability to provide effective long-term antiretroviral therapy for HIV-1 infection has become a complex issue, since 40–50% of patients who initially achieve favourable viral suppression to undetectable levels subsequently experience treatment failure [18]. Moreover, a recent study reported that viruses with resistance to at least one drug were present in 1 of 10 antiretroviral-naive patients in Europe [19]. As more drug-resistant HIV-1 isolates emerge, new classes of potent antiretroviral agents targeting different steps of the HIV replicative cycle and new combinations of agents targeting different molecules, such as gp120 and CD4 or CCR5, are a welcome addition to the HIV arsenal. CCR5 inhibitors represent a new class of agents aimed at inhibiting viral entry. Following binding of gp120 to the CD4 receptor, CCR5 antagonists inhibit the interaction of gp120 with its coreceptor, an integral step in the fusion of HIV to the host cell [6–8]. As with other antiretroviral agents, resistance will likely prove to be a problem for CCR5 inhibitors [4,20]. Thus, the best strategy for preventing the occurrence of resistance is to use them in combination with other potent antiretroviral drugs. In the present study, we found that combinations of KD-247 with CCR5 inhibitors showed very strong synergistic interactions. When both antiviral reagents become available in the near future, these combinations will represent an efficient weapon against HIV-1. However, the benefit of these combinations to patients with HIV-1 infection needs to be further evaluated in clinical trials.

Taken together, the present data suggest that KD-247 has at least five advantages: (i) it exerts potent activity against a wide spectrum of subtype B HIV-1 variants, presumably due to its interaction with the IGPGR sequence in the gp120 V3 tip; (ii) viral acquisition of KD-247-resistance requires a very high concentration of KD-247 *in vitro*; (iii) at least some representatives of each class of currently available antiretroviral agents remain active against the virus variant selected *in vitro* with KD-247; (iv) the escape variant becomes more sensitive to CCR5 inhibitors and rsCD4, and is less dependent on CD4 binding for entry; and (v) combinations of KD-247 with CCR5 inhibitors show highly synergistic interactions at all inhibitory concentrations tested to date.

Acknowledgements

We thank J. Robinson for kindly providing the 17b, S. Zolla-Pazner for kindly providing the 447-52D, and Hirotomo Nakata, Kenji Maeda and Yasuhiro Kou for technical support. We also thank Yuki Azakami for excellent technical assistance.

This work was supported in part by the Ministry of Health, Labor and Welfare of Japan (H-16-AIDS-001 and -012), Grant-in-aid for Scientific Research (C-18591119) from the Ministry of Education, Science and Culture of Japan and the Cooperative Research Project on Clinical and Epidemiological Studies of Emerging and Re-emerging Infectious Diseases.

References

1. Eda Y, Takizawa M, Murakami T, Maeda H, Kimachi K, Yonemura H, *et al.* **Sequential immunization with V3 peptides from primary HIV-1 produces cross-neutralizing antibodies against primary isolates with matching narrow neutralization sequence motif.** *J Virol* 2006; **80**:5552–5562.
2. LaRosa GJ, Davide JP, Weinhold K, Waterbury JA, Profy AT, Lewis JA, *et al.* **Conserved sequence and structural elements in the HIV-1 principal neutralizing determinant.** *Science* 1990; **249**:932–935.
3. Eda Y, Murakami T, Ami Y, Nakasone T, Takizawa M, Someya K, *et al.* **Anti-V3 humanized antibody KD-247 effectively suppresses ex vivo generation of human immunodeficiency virus type 1 and affords sterile protection of monkeys against a heterologous simian/human immunodeficiency virus infection.** *J Virol* 2006; **80**:5563–5570.
4. Yusa K, Maeda Y, Fujioka A, Monde K, Harada S. **Isolation of TAK-779-resistant HIV-1 from an R5 HIV-1 GP120 V3 loop library.** *J Biol Chem* 2005; **280**:30083–30090.
5. Cecilia D, KewalRamani VN, O'Leary J, Volsky B, Nyambi P, Burda S, *et al.* **Neutralization profiles of primary human immunodeficiency virus type 1 isolates in the context of coreceptor usage.** *J Virol* 1998; **72**:6988–6996.
6. Baba M, Nishimura O, Kanzaki N, Okamoto M, Sawada H, Iizawa Y, *et al.* **A small-molecule, nonpeptide CCR5 antagonist with highly potent and selective anti-HIV-1 activity.** *Proc Natl Acad Sci USA* 1999; **96**:5698–5703.
7. Strizki JM, Xu S, Wagner NE, Wojcik L, Liu J, Hou Y, *et al.* **SCH-C (SCH 351125), an orally bioavailable, small molecule antagonist of the chemokine receptor CCR5, is a potent inhibitor of HIV-1 infection in vitro and in vivo.** *Proc Natl Acad Sci USA* 2001; **98**:12718–12723.
8. Maeda K, Nakata H, Koh Y, Miyakawa T, Ogata H, Takaoka Y, *et al.* **Spirodiketopiperazine-based CCR5 inhibitor which preserves CC-chemokine/CCR5 interactions and exerts potent activity against R5 human immunodeficiency virus type 1 in vitro.** *J Virol* 2004; **78**:8654–8662.

9. Maeda Y, Foda M, Matsushita S, Harada S. **Involvement of both the V2 and V3 regions of the CCR5-tropic human immunodeficiency virus type 1 envelope in reduced sensitivity to macrophage inflammatory protein 1alpha.** *J Virol* 2000; **74**: 1787–1793.
10. Yoshimura K, Feldman R, Kodama E, Kavlick F, Qiu YL, Zemlicka J, *et al.* **In vitro induction of human immunodeficiency virus type 1 variants resistant to phosphoralaninate prodrugs of Z-methylenecyclopropane nucleoside analogues.** *Antimicrob Agents Chemother* 1999; **43**:2479–2483.
11. Yoshimura K, Kato R, Kavlick MF, Nguyen A, Maroun V, Maeda K, *et al.* **A potent human immunodeficiency virus type 1 protease inhibitor, UIC-94003 (TMC-126), and selection of a novel (A28S) mutation in the protease active site.** *J Virol* 2002; **76**:1349–1358.
12. Hope TJ, Huang XJ, McDonald D, Parslow TG. **Steroid-receptor fusion of the human immunodeficiency virus type 1 Rev transactivator: mapping cryptic functions of the arginine-rich motif.** *Proc Natl Acad Sci USA* 1990; **87**:7787–7791.
13. Wang FX, Kimura T, Nishihara K, Yoshimura K, Koito A, Matsushita S. **Emergence of autologous neutralization-resistant variants from preexisting human immunodeficiency virus (HIV) quasi species during virus rebound in HIV type 1-infected patients undergoing highly active antiretroviral therapy.** *J Infect Dis* 2002; **185**:608–617.
14. Chou TC, Hayball MP. *CalcuSyn*. 2nd edn. Cambridge, UK: Biosoft; 1996.
15. Chou TC, Talaly P. **A simple generalized equation for the analysis of multiple inhibitions of Michaelis–Menten kinetic systems.** *J Biol Chem* 1977; **252**:6438–6442.
16. Decker JM, Bibollet-Ruche F, Wei X, Wang S, Levy DN, Wang W, *et al.* **Antigenic conservation and immunogenicity of the HIV coreceptor binding site.** *J Exp Med* 2005; **201**:1407–1419.
17. Kuiken C, Foly B, Hahn BH, Marx P, McCutchan F, Mellors J, *et al. HIV Sequence Compendium.* Los Alamos: Los Alamos National Laboratory; 2001.
18. Richman DD. **HIV chemotherapy.** *Nature* 2001; **410**:995–1001.
19. Wensing AM, van de Vijver DA, Angarano G, Asjo B, Ballota C, Boeri E, *et al.* **Prevalence of drug-resistant HIV-1 variants in untreated individuals in Europe: implications for clinical management.** *J Infect Dis* 2005; **192**:958–966.
20. Marozsan AJ, Kuhmann SE, Morgan T, Herrera C, Rivera-Troche E, Xu S, *et al.* **Generation and properties of a human immunodeficiency virus type 1 isolate resistant to the small molecule CCR5 inhibitor, SCH-417690 (SCH-D).** *Virology* 2005; **338**: 182–199.

MAJOR ARTICLE

Recurrent HIV-1 Integration at the *BACH2* Locus in Resting CD4$^+$ T Cell Populations during Effective Highly Active Antiretroviral Therapy

Terumasa Ikeda, Junji Shibata, Kazuhisa Yoshimura, Atsushi Koito, and Shuzo Matsushita

Division of Clinical Retrovirology and Infectious Diseases, Center for AIDS Research, Kumamoto University, Kumamoto, Japan

The persistence of latent human immunodeficiency virus type 1 (HIV-1) has been considered one of the major obstacles for eradication of the virus in infected individuals receiving successful antiretroviral therapy. To determine the contribution of integration sites to viral latency within clinical settings, an inverse polymerase chain reaction method was used to analyze integration sites in CD4$^+$ T cells from patients showing long-term undetectable plasma viral RNA. Of 457 sites identified in 7 patients, almost all (96%) resided within transcriptional units, usually in introns of the human genome. Studies of 18 genes in which HIV-1 integrates found them to be actively expressed in resting CD4$^+$ T cells. On the other hand, integration sites in the α satellite region was also identified in some patients, albeit at low frequency. Of particular interest, HIV-1–infected cells with multiple identical integration sites were detected in longitudinal analysis of samples from 3 patients, suggesting that these cells persist for long periods and that clonal expansion may occur. Furthermore, strong integration clusters in the *BACH2* gene were observed in 2 patients (31% in patient 1 and 5% in patient 3). Our findings not only raise the possibility of biased target-site integration but also provide mechanistic insights into the long-term persistence of HIV-1.

The development of highly active antiretroviral therapy (HAART) for the treatment of HIV-1 infection has allowed the complete suppression of detectable viremia in adherent patients. However, the presence of latently infected resting CD4$^+$ T cells has been consistently demonstrated in the majority of these individuals [1–8], and the persistence of this latent reservoir is considered to be a major obstacle for successful eradication of HIV-1 in infected individuals receiving HAART [2, 5, 8–11].

Received 7 July 2006; accepted 22 September 2006; electronically published 18 January 2007.

Potential conflicts of interest: none reported.

Financial support: Ministry of Health, Labor, and Welfare of Japan (grant H16-AIDS001); Cooperative Research Project on Clinical and Epidemiological Studies of Emerging and Reemerging Infectious Diseases of the Ministry of Education, Culture, Sports, Science, and Technology of Japan (grant 78 to Kumamoto University).

Reprints or correspondence: Dr. Shuzo Matsushita, Div. of Clinical Retrovirology and Infectious Diseases, Center for AIDS Research, Kumamoto University, Kumamoto 860-0811, Japan (shuzo@kaiju.medic.kumamoto-u.ac.jp).

The Journal of Infectious Diseases 2007;195:716–25

0022-1899/2007/19505-0018$15.00

DOI: 10.1086/510915

Latent infection of CD4$^+$ T cells may occur through 2 mechanisms, both of which are operative only in cells that are in a resting G_0 state [8]. Partially or completely reverse-transcribed HIV-1 DNA is present in the cytoplasm of infected resting CD4$^+$ T cells as a result of a block in reverse transcription or nuclear import and constitutes a labile, inducible reservoir [12, 13]. A second, more stable latent reservoir is composed of resting memory CD4$^+$ T cells with integrated provirus [2, 8, 12, 14]. The frequency of these cells is extremely low. Although a fraction of them harbors replication-competent provirus [2–6,10, 12], these T cell populations generally do not release virus unless the cells are stimulated in some manner [3, 6, 12]. Because the biological function of memory cells is to persist for long periods of time to allow responses to previously encountered antigens and because the viral DNA in these cells is stably integrated, these latently infected memory cells can potentially serve as a long-term reservoir for HIV-1 [15].

HIV-1 latency likely results not from a complete block at any single step in replication but rather from

Table 1. Clinical characteristics of the patients with HIV-1 infection.

Patient (sex)	HIV-1 subtype	Baseline data (before therapy)			Therapy	Recent data (~2005)			Time receiving HAART with <50 copies/mL, months	Duration of therapy, months	Present therapy regimen
		Viral load, copies/mL	$CD4^+$ cell count, cells/μL	pDNA load, copies/10^6 PBMCs		Viral load, copies/mL	$CD4^+$ cell count, cells/μL	pDNA load, copies/10^6 PBMCs			
1 (M)	B	3200	658	75	Sep 1998	<50	799	14	83	84	NFV + AZT + 3TC
2 (M)	B	>100,000	190	159	Sep 1996	<50	389	11	105	108	LPV/r + AZT + 3TC
3 (M)	B	37,000	394	463	Jun 2000	<50	1254	84	57	62	SQV + RTV + AZT + 3TC
4 (M)	B	45,000	2	ND	Jan 1997	<50	702	157	50	100	LPV/r + EFV + ABC + 3TC
5 (M)	B	>100,000	340	531	Feb 2002	<50	612	14	42	44	LPV/r + AZT + 3TC
6 (F)	CRF01	12,000	279	73	Nov 1998	<50	1220	16	80	82	LPV/r + AZT + 3TC
7 (F)	B	31,000	137	114	Apr 2000	<50	622	19	60	64	SQV + RTV + d4T + 3TC
Mean	...	...	286	236	...	<50	800	45	68	78	...

NOTE. 3TC, lamivudine; ABC, abacavir; AZT, zidovudine; d4T, stavudine; ddI, didanosine; EFV, efavirenz; F, female; LPV/r, lopinavir/ritonavir; M, male; ND, not determined; NFV, nelfinavir; PBMCs, peripheral-blood mononuclear cells; pDNA, proviral DNA; RTV, ritonavir; SQV, saquinavir.

Table 2. Primers used for polymerase chain reaction.

The table is available in its entirety in the online edition of the *Journal of Infectious Diseases*.

partial defects at multiple steps. Although molecular mechanisms of HIV-1 latency have been proposed [8], there has been no conclusive identification of host factors that direct a T lymphocyte to become latent. After integration into a nonrandom position within the human genome [16], HIV-1 is thought to establish a low basal expression rate that depends on the integration site [17, 18]. Integrated provirus is joined to flanking cellular DNA at exactly the same points at the ends of the viral DNA, but integration takes place at many different sites in the host cell chromosomes. Thus, the viral genome provides a homogenous transcription template that can be analyzed at different chromosomal locations, allowing the influence of flanking chromosomal features to be assessed [19, 20]. This finding has fueled increased interest in assessing the relationship between HIV-1 persistence and integration sites.

There has been considerable interest in the idea that the nonproductive state of the viral reservoirs may reflect proviral integration into chromosomal sites that repress transcription or that can result in transcriptional repression [17, 18]. On the other hand, it was recently reported that the absence of virus production in resting $CD4^+$ T cells with integrated HIV-1 DNA could not be attributed to integration into chromosomal regions that intrinsically repress transcription [21]. Furthermore, transcriptional initiation and elongation have been shown to occur at low levels in infected resting $CD4^+$ T cells [7]. However, the involvement of integration sites in residual viruses in clinical settings remains controversial.

In the present study, integration sites were cloned using an inverse polymerase chain reaction (PCR) method and were mapped by sequencing junctions between proviral and host-cell DNA, and their positions in the human genome were explored. We report that the nonproductive nature of residual viruses in $CD4^+$ T cells obtained from patients showing long-term (5–8 years) undetectable plasma viral RNA because of HAART does not appear to be related to the characteristics of the integration sites. Furthermore, in circulating $CD4^+$ T cells from 2 patients, we observed a long-term high incidence of accumulation of integration sites in the *BACH2* gene locus.

PATIENTS, MATERIALS, AND METHODS

Study patients. Peripheral-blood mononuclear cells (PBMCs) were obtained from 7 patients without viremia (patients 1–7) who had achieved suppression of plasma HIV-1 RNA levels to <50 copies/mL for >42 months with antiretroviral combination therapy (table 1). The blood samples were used for $CD4^+$ T cell counts, measurement of HIV-1 RNA in plasma, and measurement of proviral HIV-1 DNA (pDNA). $CD4^+$ T cell counts were measured using flow cytometry by standard procedures. Plasma HIV-1 RNA levels were measured using the ultrasensitive HIV-1 Amplicor Monitor assay (Roche Diagnostics), which has a detection limit of 50 HIV-1 RNA copies/mL. HIV pDNA was measured using HIV Gag primers and probe and an ABI PRISM 7000 sequence detection system (PerkinElmer–

Table 3. Chromosomal features associated with HIV-1 integration sites in infected $CD4^+$ T cells.

Chromosomal feature	Percentage in human genome	Integration sites, %			
		Patient 1 (n = 14)	Patient 2 (n = 56)	Patient 3 (n = 86)	Patients 4–7 (n = 15)
Transcriptional units	~33[a]	92.9[b]	94.6[b]	96.5[b]	86.7[b]
Intron		92.3	96.2	100.0	100.0
Exon		7.7	3.8	0.0	0.0
SINEs					
Alu	10.6	0.0	21.4[c]	25.6[b]	6.7
MIR	2.2	0.0	5.4	3.5	0.0
DNA elements	2.8	0.0	3.6	1.2	6.7
LTR elements	8.3	0.0	3.6	4.7	0.0
LINEs	20.0	35.7	14.3	10.5[c]	13.3
α satellite	UN	0.0	1.8	1.2	6.7

NOTE. The integration sites studied included those mapped to unique locations on the genome and those in identifiable repeats. *P* values are for the comparison of each integration site population to the human genome. LINEs, long interspersed nuclear elements; LTR, long terminal repeat; MIR, mammalian-wide interspersed repeat; SINEs, short interspersed nuclear elements; UN, unknown.

[a] Estimated value.

[b] $P < .001$.

[c] $P < .01$.

Table 4. Distribution of HIV-1 integration sites in the human genome in longitudinal samples obtained from patients 1, 2, and 3.

Chromosomal feature	Patient 1 integration sites, %					Patient 2 integration sites, %			Patient 3 integration sites, %	
	Jul 1998 (n = 46)	Jul 1999 (n = 53)	Aug 2000 (n = 63)	Nov 2002 (n = 21)	Dec 2004 (n = 14)[a]	Apr 1998 (n = 24)	Nov 2002 (n = 69)	Nov 2004 (n = 56)[a]	Apr 2001 (n = 10)	Feb 2005 (n = 86)[a]
Transcriptional units	97.8[b]	96.2[b]	98.4[b]	95.2[b]	92.9[b]	100.0[b]	92.8[b]	94.6[b]	100.0[b]	96.5[b]
Intron	97.8	96.1	93.7	95.0	92.3	91.7	96.9	96.2	100.0	100.0
Exon	2.2	3.9	4.8	0.0	7.7	4.2	0.0	3.8	0.0	0.0
SINEs										
Alu	10.9	20.8[c]	20.6[b]	23.8[c]	0.0	20.8	8.7	21.4[d]	20.0	25.6[b]
MIR	0.0	1.9	0.0	0.0	0.0	4.2	2.9	5.4	0.0	3.5
DNA elements	13.0[d]	1.9	6.3	0.0	0.0	4.2	2.9	3.6	0.0	1.2
LTR elements	4.3	5.7	3.2	4.8	0.0	8.3	2.9[c]	3.6	10.0	4.7
LINEs	34.8[d]	26.4	19.0	33.3	35.7	41.7[d]	21.7	14.3	0.0	10.5[d]
α satellite	0.0	0.0	1.6	0.0	0.0	0.0	1.4	1.8	0.0	1.2

NOTE. The integration sites studied included those mapped to unique locations on the genome and those in identifiable repeats. *P* values are for the comparison of each integration site population to the human genome. LINEs, long interspersed nuclear elements; LTR, long terminal repeat; MIR, mammalian-wide interspersed repeat; SINEs, short interspersed nuclear elements.

[a] The integration sites at this point are described in table 3.
[b] $P < .001$.
[c] $P < .05$.
[d] $P < .01$.

Applied Biosystems), as described elsewhere [22]. Under these conditions, the detection limit for pDNA was 10 copies/1 × 10^6 PBMCs. The present study was conducted under the approval of the Institutional Review Board of the Kumamoto University Hospital, Japan. Informed consent was obtained from all patients.

Purification of CD4⁺ T cells. PBMCs from the patients were prepared by use of Ficoll-Paque (Ficoll-Paque PLUS; Amersham Pharmacia Biotech AB) density centrifugation. $CD4^+$ T cells were negatively isolated by use of the $CD4^+$ T Cell Isolation Kit II (Miltenyi Biotec). The resulting purity of the $CD4^+$ T cell populations was ~98%.

Analysis of HIV-1 integration sites. Analysis of integration sites was performed by an inverse PCR method [21], with minor modifications. To increase the efficiency of inverse PCR, circularized DNA was cleaved by use of *Afl*II (NEB) at nt 517, which is conserved in clade B isolates [23]. The linearized DNA was diluted and amplified with sets of primers that have been

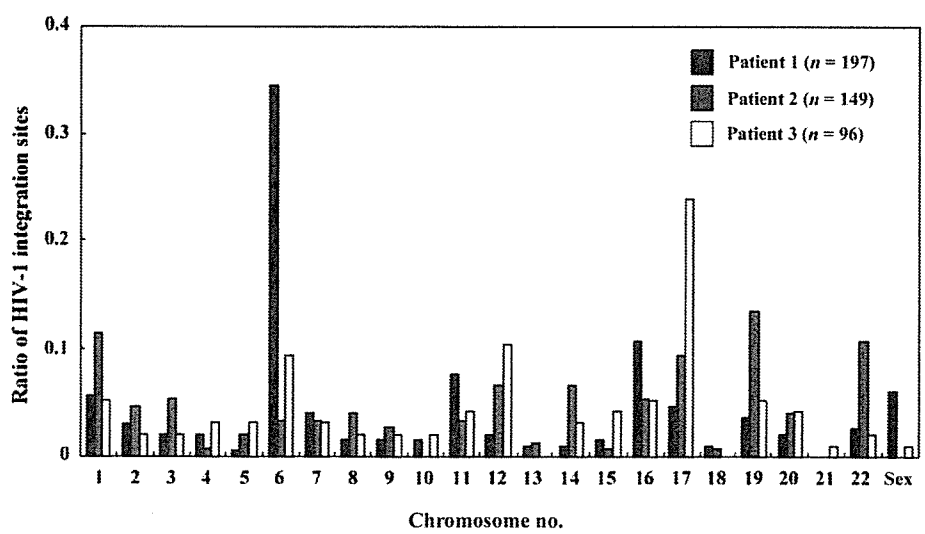

Figure 1. Frequency of HIV-1 integration in the human genome. Human chromosome nos. are indicated on the horizontal axis of the figure. The percentage of integration events detected in each chromosome against total integration events is indicated on the vertical axis. Black bars indicate HIV-1 integration sites in peripheral-blood mononuclear cells (PBMCs) from patient 1, gray bars indicate sites in PBMCs from patient 2, and white bars indicate sites in PBMCs from patient 3. Higher bars indicate favored integration.

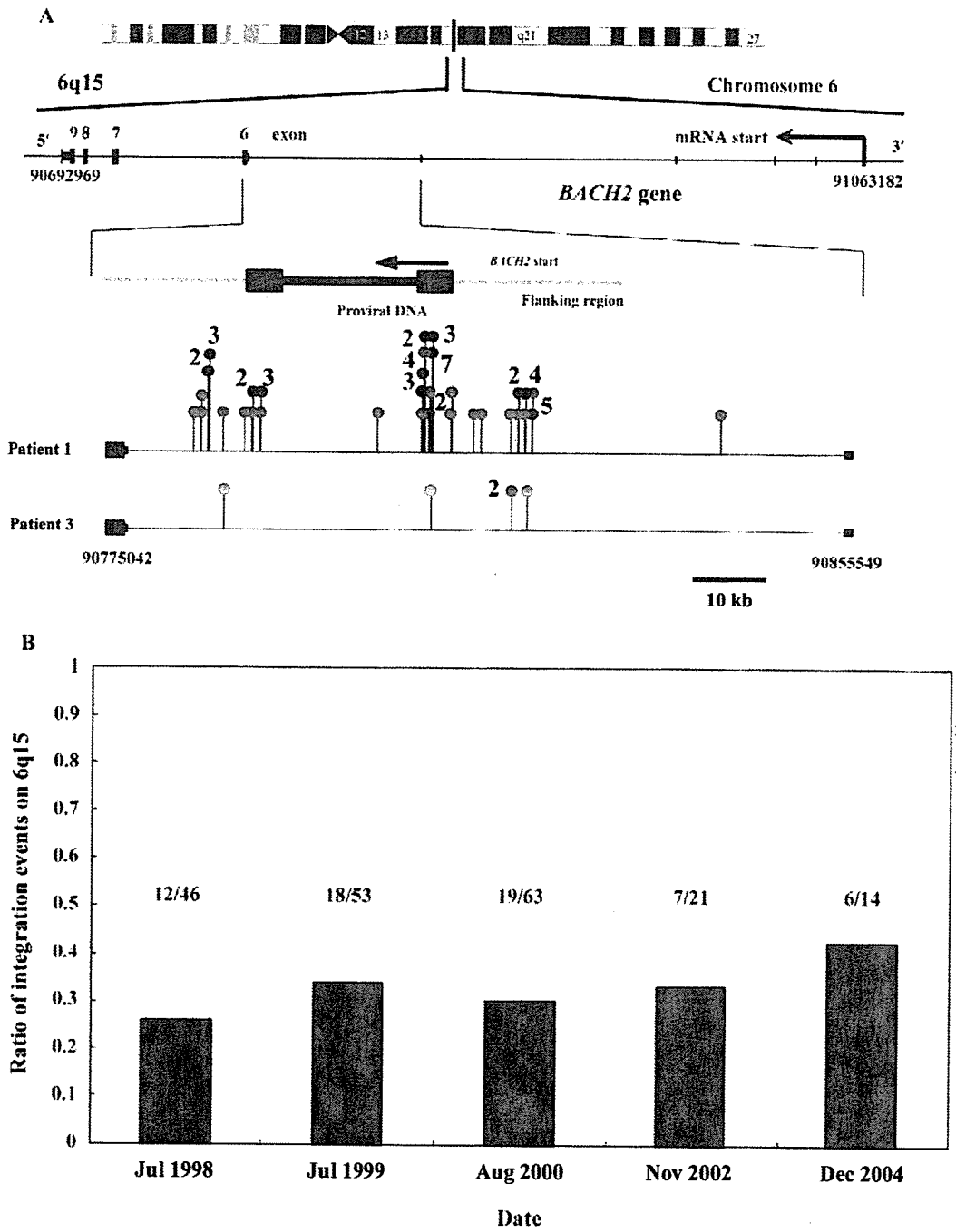

Figure 2. The regional hotspot for HIV-1 integration on chromosome 6q15 (*BACH2* gene). *A,* Exon-intron structure of the human *BACH2* gene. The human *BACH2* gene, the direction of which is indicated by the arrow, is composed of 9 exons, of which 4 are coding (indicated by red boxes) and 5, located at the 5′ end of the gene, are noncoding. Thirty-one percent and 5% of the HIV-1 integration sites were located within the fifth intron of the *BACH2* gene in patients 1 and 3, respectively. Transcriptional orientation of all integrated HIV-1 sequences were the same as the direction of the *BACH2* gene, as indicated by the arrow. The relative locations of the chromosomal sequences matching the HIV-1 integration sites are shown as lollipops above the linear chromosomes. Green and purple coloration indicate integration events on the locus identified in peripheral-blood mononuclear cells (PBMCs) from patient 1; green indicates the detection of single integration events at 5 points during the course of HIV infection under highly active antiretroviral therapy (HAART), and purple indicates that the integration site was detected several times, as indicated by the no. above. Yellow and orange indicate the integration events for the locus identified in PBMCs from patient 3; yellow indicates the detection of a single integration event, and orange indicates the detection of 2 integration events. *B,* Concentration of integration sites on the *BACH2* gene locus in patient 1. This experiment was done at 5 different time points during the course of HIV infection under HAART.

Table 5. HIV-1 integration sites identified on multiple occasions by longitudinal analysis.

The table is available in its entirety in the online edition of the *Journal of Infectious Diseases*.

described elsewhere [21]. The nested reaction–produced bands, visible on agarose gels, were eluted and directly sequenced. By use of the University of California, Santa Cruz, Bioinformatics Human Genome Database (available at: http://www.genome.ucsc.edu; May 2004 assembly), the human genomic sequence in each inverse PCR fragment was identified. The matched sequence was judged to be authentic only if a match to the human genome (1) joined directly to the end of the 5′ long terminal repeat (LTR) of HIV-1 (5′-TG-3′) and (2) yielded a unique best-hit Blat ranking (>95%).

Analysis of gene expression in resting CD4⁺ T cells by reverse-transcriptase (RT)–PCR. Resting $CD4^+$ T cells were purified by use of a method described elsewhere [24]. Briefly, $CD4^+$ T cells in PBMCs from a healthy donor or patient 1 were isolated by negative selection, as described above. The fraction of $CD4^+$ T cells was further depleted of $CD25^+HLA\text{-}DR^+$ cells by direct immunomagnetic conjugation ($CD4^+CD25^-HLA\text{-}DR^-$ T cells; resting $CD4^+$ T cells). The purified resting $CD4^+$ T cells showed <1% contamination with activated cells. The $CD45RO^+CD45RA^-$ subset of resting $CD4^+$ T cells (resting memory $CD4^+$ T cells) was isolated by including anti-CD45RA antibody in the initial depletion. The purity of these populations was >99%.

Total cellular RNA was isolated using the RNeasy Kit (Qiagen). RNA was treated with DNase (Qiagen) and then reverse transcribed into cDNA by use of a High-Capacity cDNA Archive Kit (Applied Biosystems). The primers used are shown in table 2. The amplification conditions were as follows: 94°C for 1 min; 30 cycles at 98°C for 10 s, 62°C for 30 s, and 72°C for 20 s; and final extension at 72°C for 7 min. In each experiment, control reactions from which RT was omitted were run to ensure that genomic DNA was not amplified.

Analysis of activated PBMCs from patients. PBMCs were isolated from HIV-1–positive donors who had achieved suppression of plasma viremia to <50 copies/mL while receiving HAART. The PBMCs were depleted of $CD8^+$ T cells (hereafter, "CD8-depleted PBMCs") by binding with magnetic beads conjugated with anti-CD8 antibody (CD8 Dynabeads; Dynal). CD8-depleted PBMCs were cultured in RPMI 1640 medium with 10% fetal calf serum at 37°C for a week in the presence of anti-CD3 antibody (1 μg/mL) and human recombinant interleukin-2 (20 IU/mL; Genzyme). On days 5 and 7 of culture, HIV-1 p24 antigen in the culture supernatants was measured by ELISA (ZeptoMetrix). On day 7 of culture, total RNA was isolated from CD8-depleted PBMCs, and the RNA was treated with DNase and then reverse transcribed. The cDNA from multiply spliced (MS), singly spliced (SS), and unspliced (US) HIV-1 RNA in CD8-depleted PBMCs was amplified with primers in each conserved region shown in table 2 [23].

PCR conditions for MS RNA (first PCR) were 94°C for 1 min; 30 cycles at 98°C for 10 s, 62°C for 30 s, and 72°C for 1.5 min; and a final extension at 72°C for 7 min. PCR conditions for MS RNA (second PCR) and SS and US RNA (first PCR) were 94°C for 1 min; 30 cycles at 98°C for 10 s, 62°C for 30 s, and 72°C for 1 min; and a final extension at 72°C for 7 min. PCR conditions for SS and US RNA (second PCR) were 94°C for 1 min; 30 cycles at 98°C for 10 s, 62°C for 30 s, and 72°C for 30 s; and a final extension at 72°C for 7 min. PCR products were cloned and sequenced.

Nucleotide sequence accession numbers. The sequences determined in the present study have been submitted to GenBank and were assigned accession numbers AB256049–AB256512.

RESULTS

Our study cohort consisted of 7 HIV-1–infected patients who achieved long-term suppression of plasma viremia by HAART (table 1). All patients were treated for a median of 78 months (range, 62–108 months), and the median time with a viral load <50 copies/mL was 68 months (range, 42–105 months). The baseline and recent median $CD4^+$ T cell counts were 286 cells/μL (range, 2–658 cells/μL) and 800 cells/μL (range, 389–1254 cells/μL), respectively. Detectable levels of HIV DNA in PBMCs (pDNA) were found in all patients, with a median value of 236 (range, 73–531) and 45 (range, 11–157) copies/1 × 10^6 PBMCs at the baseline and recent-data time points, respectively. Even though the number of patients analyzed is limited, these data do suggest that a decline in pDNA level is achievable even in chronically infected patients by continuation of HAART.

Residence of most HIV-1 DNA integration sites in transcriptional units. We characterized a total of 171 integration sites in bulk $CD4^+$ T cells from 7 patients (table 3) after prolonged viral suppression. Of the integrated viral genomes, 162 were found to reside within transcriptional units. Among them, 82% of the integration sites were located within RefSeq genes, which are a set of well-annotated genes based on mRNA records [25]. Because only ~33% of the human genome are transcriptional units [26], this analysis of HIV-1 integration sites in vivo in $CD4^+$ T cells revealed a highly significant departure from that expected as a result of random insertion ($P < .001$). Of the 162 integration sites residing within genes, 159 (98%) were in introns. Thus, consistent with previous observations [21], HIV-1 integration sites in patients who had received prolonged and effective HAART accumulated in the introns within genes.

Longitudinal analysis of integration sites in patients with prolonged viral suppression. To examine the relationship between latent HIV-1 infection and integration sites over time in

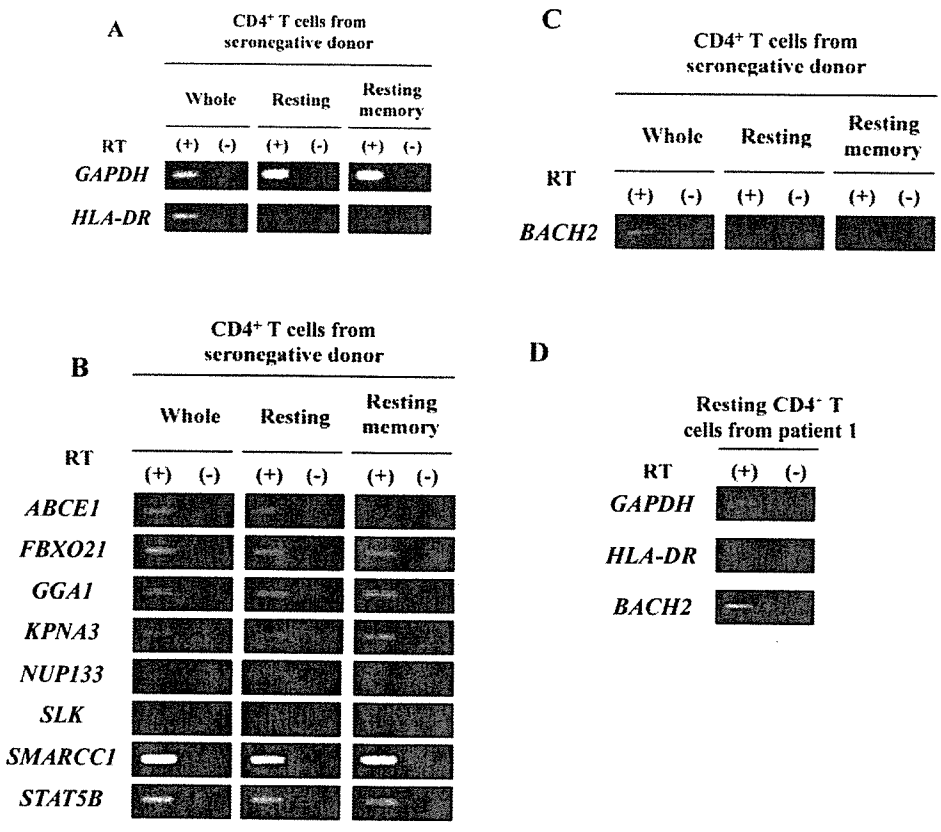

Figure 3. Analysis of host gene expression in resting CD4+ T cells. *A*, Patterns of mRNA expression of *GAPDH* and *HLA-DR* in whole, resting, and resting memory CD4+ T cells from a seronegative donor. *GAPDH* served as a positive control for reverse-transcriptase polymerase chain reaction (RT-PCR) and *HLA-DR*, as did activated CD4+ T cells. Samples prepared without RT were used to ascertain that the PCR signals were derived from RNA, not from contaminating DNA. *B*, Expression of 18 genes targeted for HIV-1 integration in peripheral-blood mononuclear cells or CD4+ T cells from a seronegative donor were analyzed in triplicate by RT-PCR. Representative examples of 8 genes (*ABCE1, FBXO21, GGA1, KPNA3, NUP133, SLK, SMARCC1,* and *STAT5B*) are shown. *C*, Analysis of expression of *BACH2*, which had regional hotspots for HIV-1 integration, in resting and resting memory CD4+ T cells from a seronegative donor. *D*, *BACH2* mRNA expression in resting CD4+ T cells from patient 1.

patients receiving prolonged and effective HAART, we analyzed 442 integration sites in PBMC samples from 3 patients obtained at several points during the clinical course. Most integrated pDNA in these longitudinal samples were found in transcriptional units, predominantly in the introns within the human genome (table 4). Therefore, most HIV-1 integration sites remained in transcriptional units during the clinical course with HAART despite a reduction in pDNA level. In all patients, only 5 (1.1%) of the 457 integration sites analyzed were distributed in α satellites, corresponding to the heterochromatin region.

Regional hotspots for integration of residual HIV-1. We next examined the distribution of integration sites on each chromosome in the 3 patients. As shown in figure 1, the frequencies of integration in the different chromosomes were quite different. For example, chromosome 19 was the most frequent integration site in patient 2, and chromosome 17 was the most frequent integration site in patient 3. It has been reported that HIV-1 prefers to integrate into these 2 chromosomes, and this phenomenon correlates with the high gene densities [27, 28]. In patient 1, on the other hand, 35% (68/197) of the integration events were concentrated in chromosome 6, which is a relatively gene-poor chromosome [29]. Moreover, almost all of these integration events (62/68 [91%]) accumulated in the *BACH2* gene, and 4 local hotspots on the fifth intron of the *BACH2* gene were identifiable by the method described by Schröder et al. [16] (figure 2*A*). Integration into this gene locus can be detected throughout the clinical course of HAART in patient 1 (figure 2*B*). We also found integration events in the *BACH2* gene in patient 3 (5/96 [5%]), whereas no such integration events were found in the other patient. We checked all the proviral plasmids and HIV-1–infected cell lines in our laboratory for their flanking sequences. None of them had a sequence that matched the *BACH2* locus.

Furthermore, identical integration sites were frequently detected within the *BACH2* gene in patient 1 (figure 2*A*). The identical integration sites in the *BACH2* gene were observed